Self-organising coordinate transformation with peaked and monotonic gain modulation in the primate dorsal visual pathway

Daniel M. Navarro[1,2*], Bedeho M. W. Mender[1], Hannah E. Smithson[2], Simon M. Stringer[1]

1 Oxford Centre for Theoretical Neuroscience and Artificial Intelligence, Department of Experimental Psychology, University of Oxford, South Parks Road, Oxford, Oxfordshire, United Kingdom
2 Oxford Perception Lab, Department of Experimental Psychology, University of Oxford, South Parks Road, Oxford, Oxfordshire, United Kingdom

* daniel.navarro@psy.ox.ac.uk

Abstract

We study a self-organising neural network model of how visual representations in the primate dorsal visual pathway are transformed from an eye-centred to head-centred frame of reference. The model has previously been shown to robustly develop head-centred output neurons with a standard trace learning rule [1], but only under limited conditions. Specifically it fails when incorporating visual input neurons with *monotonic* gain modulation by eye-position. Since eye-centred neurons with monotonic gain modulation are so common in the dorsal visual pathway, it is an important challenge to show how efferent synaptic connections from these neurons may self-organise to produce head-centred responses in a subpopulation of postsynaptic neurons. We show for the first time how a variety of modified, yet still biologically plausible, versions of the standard trace learning rule enable the model to perform a coordinate transformation from eye-centred to head-centred reference frames when the visual input neurons have monotonic gain modulation by eye-position.

Author summary

Coordinate transformations are an essential aspect of behaviour. For instance, sensory information encoded in the coordinates of the retina needs to be transformed to relevant coordinates for planning and movement. Particularly, head-centred coordinates are essential for accurate motor behaviours and required to compute more complex coordinate transformations for sensorimotor integration [2]. Head-centred coordinates are obtained by combining information about the the retinal location of visual stimuli and the position of the eye. Previous work did not address the influence of different forms of gain modulation by eye position, albeit a variety of forms being widely reported for several cortical areas. Here we show how a biologically plausible model that successfully self-organised head-centred responses [1,3] fails when the visual input units have a commonly observed form of eye-position gain modulation, i.e. *monotonic modulation*. Our work makes an important contribution to understanding how head-centred responses may develop in the brain through an unsupervised process of visually-guided learning using a set of more sophisticated, and yet still biologically

plausible, learning rules when visual precursor neurons have monotonic eye-position
gain modulation. Furthermore, our findings may be applied to a range of other
coordinate transformations with sensorimotor integration of monotonically encoded
motor variables [4,5].

Introduction   1

Within the primate dorsal visual pathway, neurons encode the locations of visual   2
objects in different body-centred frames of reference. For example, neurons at an early 3
stage of processing encode the locations of objects within an eye-centred reference   4
frame, while neurons in later stages may encode the positions of objects with respect to 5
the head or hand which is more relevant for guiding motor actions. A key question is   6
how the visual system learns to perform such coordinate transformations between   7
different body-centered reference frames. The neural mechanisms supporting this form   8
of transformation, critical for visually guided motor function, have long been studied in 9
primates. A neural phenomenon which is thought to play a key role in coordinate   10
transformations in the dorsal visual pathway is *gain modulation*. This refers to the   11
modulatory effect that a particular bodily state or posture, like eye or head position,   12
has on the firing rate of some visual neurons responding in a given reference frame.   13
Gain modulation of neuronal firing responses has been discovered in multiple stages of 14
the primate dorsal visual pathway.   15

Parietal area 7a [6,7], LIP [8] and PO [9] have visual neurons modulated by the   16
position of the eye in the orbit. This form of gain modulation is thought to be involved 17
in supporting the development of head-centred visual representations, which were later 18
identified in the same areas [10–12]. The parietal reach region (PRR) has hand-centred 19
visual neurons with eye-position gain modulation [5], which are thought to be involved 20
in guiding reaching to target locations. In certain regions such as parietal area 7a and 21
LIP, the gain modulation is usually a *monotonic* function of the relevant bodily posture, 22
such as eye or head position. For example, eye-position modulation often takes the form 23
of a linear or saturating function of eye-position, which multiplicatively modulates the 24
underlying Gaussian retinotopic receptive field of a visually responsive neuron [6].   25
While in other areas, such as V6A, there can be a higher proportion of retinotopic   26
visual neurons with peaked eye-position gain fields [13].   27

Contemporary understanding of the potential role of such gain modulation in   28
coordinate transformation has been informed by the highly influential coordinate   29
transformation model of [14], reviewed below (section Previous Neural Network Models). 30
The majority of models studying coordinate transformation since that time [4,5,15–17] 31
have been heavily inspired by this early work. These models set up the synaptic weight 32
matrix by some form of supervised, error correction, learning algorithm which cannot be 33
implemented in the cortex [18]. Such algorithms provide no biologically plausible   34
learning hypothesis, and also produce circuits which violate Dale's law, the widely   35
accepted neuroanatomical fact that a given presynaptic neuron cannot be both   36
excitatory and inhibitory across its efferent synapses [19].   37

Our laboratory has developed a biologically plausible neural network model that   38
self-organises its synaptic connectivity during visual experience such that the model   39
learns to transform eye-centred visual representations to head-centred   40
representations [1,3]. The model can achieve this using purely associative local synaptic 41
learning rules with no supervisory training signal - i.e. unsupervised learning. The   42
model is able to self-organise its synaptic connectivity by exploiting the natural eye and 43
head movements of primates. However, a limitation of previous studies with this model 44
has been their reliance on incorporating retinotopic visual input neurons with responses 45
that are modulated by only *peaked* eye-position gain fields. This is not biologically   46

realistic because many retinotopic visual neurons in the monkey brain are found to have $\quad$ 47
monotonic eye-position gain fields. In the new simulations presented below, we first $\quad$ 48
show that the incorporation of retinotopic visual input neurons with monotonic gain $\quad$ 49
fields leads to a failure of the model to develop head-centred output neurons. We then $\quad$ 50
show how model performance can be substantially improved by employing a range of $\quad$ 51
more sophisticated, yet still biologically plausible, learning rules. $\quad$ 52

Next we present a review of relevant physiological and behavioural data along with a $\quad$ 53
discussion of some previous computational models in order to provide the context for $\quad$ 54
the new simulation results discussed in this paper. $\quad$ 55

Physiology $\quad$ 56

Eye-Position gain modulation of retinotopic visual neurons in parietal $\quad$ 57
cortex $\quad$ 58

Computer simulations carried out within our laboratory have demonstrated that an $\quad$ 59
important precursor to the emergence of head-centred visual neurons in the parietal $\quad$ 60
cortex is likely to be the presence of retinotopic visual neurons with responses that are $\quad$ 61
gain modulated by the position of the eye in the orbit [1,3]. A number of experimental $\quad$ 62
studies have previously confirmed the existence of such retinotopic visual neurons with $\quad$ 63
eye-position gain fields in the monkey brain. $\quad$ 64

The work by [6] was the earliest demonstration of the influence of the position of the $\quad$ 65
eye in the orbit on the responses of retinotopic light sensitive neurons in area 7a of the $\quad$ 66
monkey parietal cortex. The authors studied the responses of light sensitive neurons $\quad$ 67
using both an attentive task and an inattentive task. In both tasks, the position of the $\quad$ 68
head was kept fixed while the animal was able to move its eyes. During the attentive $\quad$ 69
task the monkey had a peripheral stimulus flashed in a particular eye-centred location $\quad$ 70
whilst maintaining fixation at some gaze angle. Conversely, during the inattentive task $\quad$ 71
targets were flashed on random locations of the screen whilst the monkey freely oriented $\quad$ 72
its gaze. The authors reported that the position of the eyes in the socket affected the $\quad$ 73
responses of neurons in area 7a of the inferior parietal lobule during both attentive $\quad$ 74
fixation and under the inattentive condition. Although it was also found that the $\quad$ 75
responses of a much larger proportion of neurons were modulated by eye position during $\quad$ 76
the attentive task than the inattentive task. The first task, the attentive task, revealed $\quad$ 77
that 61% of neurons had their responses to visual stimuli significantly changed by the $\quad$ 78
eye position. The neuronal responses could be more than three times stronger when the $\quad$ 79
eye position shifted by 20° towards the preferred direction (optimal eye position). The $\quad$ 80
second task, the inattentive task, revealed that a significantly smaller proportion of $\quad$ 81
examined neurons (10%) had their responses to visual stimuli significantly changed by $\quad$ 82
the eye position. The precise interaction between the visual signal encoding the $\quad$ 83
retinotopic location of the target and the eye position signal was later characterized $\quad$ 84
by [7]. These effects were also observed in the lateral intraparietal area (LIP) by [8]. $\quad$ 85
This later work described such gain modulated responses as a multiplicative interaction $\quad$ 86
between a Gaussian retinotopic receptive field and a *monotonic* (planar) eye position $\quad$ 87
modulation component. $\quad$ 88

The presence of more *peaked* eye position gain modulation has been observed in the $\quad$ 89
parietal occipital area (PO) by [9] and [13]. In the more recent of these two studies, [13] $\quad$ 90
designed an experimental task to investigate the proportion of retinotopic visual neurons $\quad$ 91
in area V6A of the primate brain that are modulated by eye position with either peaked $\quad$ 92
(non-monotonic) or planar (monotonic) gain fields. During the experimental task the $\quad$ 93
monkey had 9 equally spaced fixation locations organised as a 3×3 grid, with the $\quad$ 94
visual stimulus always presented at the fixation point. These authors found that $\quad$ 95
approximately 56% of recorded neurons had their responses modulated by the position $\quad$ 96

of the eye. Furthermore, 27% of the neurons with responses that were modulated by eye position had planar gain fields, whilst the remaining 73% had peaked gain fields. The authors also explored the influence of each type of gain modulation on a traditional neural network model of sensorimotor transformation proposed by [20]. Their main motivation was to understand the implications of the functional form of gain fields, i.e. peaked (non-monotonic) *vs* planar (monotonic), for sensorimotor transformations in reaching tasks. In particular, they investigated how the functional form of the gain fields affected the performance of the model proposed by [20] to transform eye-centred visual representations into head-centred representations. The authors found that the incorporation of planar rather than peaked eye-position gain fields led to reduced model performance, with the population of output neurons providing a less accurate representation of the location of the visual stimulus with respect to the head.

Head-centred neural responses

A number of experimental studies have found visual neurons in the monkey brain that encode the locations of visual stimuli with respect to the head, i.e. within a head-centred frame of reference. The model simulations that we present below in section Results seek to explain how such head-centred neurons may develop in the brain.

[11] was the first experimental study to provide evidence of head-centred visual representations in the preoptic area (PO) of the macaque brain. A head-centred representation of visual space is assumed to be important for visually guided reaching and perceptual stability. In fact, [21] had previously predicted the existence of head-centred visual neurons in PO due to the presence of retinotpic visual neurons with eye-position gain modulation in areas 7a [7], LIP [8] and V3A [21], which are a key precursor to the development of head-centred visual representations [1,3]. In the experimental study of [11], a head-restrained monkey performed a series of fixations to different locations on a screen whilst a visual target was presented in various other screen locations for each fixation. This allowed the authors to assess how individual neuron's activity depended on either the eye-centred or head-centred location of the visual target. It was reported that the receptive fields of 11% of recorded neurons were not completely eye-centred, with six of these neurons presenting clear head-centred receptive fields. The authors concluded that previous claim by [8] that there was no explicit head-centred neuronal representation of visual space was incorrect. Furthermore, head-centred neurons were suggested to originate from pooling the output of preceding eye-position gain-modulated retinotopic visual neurons.

The work of [10] was motivated by the behavioural requirement for the brain to be able to integrate visual and auditory signals, such as the sight of moving lips and the corresponding speech sound, within a common body-centred frame of reference. The authors' investigation of the reference frames used to encode visual and auditory responses in area LIP revealed the first head-centred visual representations in this area. This contradicted the suggestion made by [8] that head-centred responses would not exist in area LIP. The proportion of neurons sensitive to visual target locations was 72%, whilst 51.4% of neurons were sensitive to auditory target locations. Moreover, 5% to 43% of neurons were simultaneously responsive to both visual and auditory target locations, depending on how responsiveness was defined. For visual neurons, 33% had eye-centred responses and 18% had head-centred responses. Regarding auditory neurons, 10% had eye-centred responses while 23% had head-centred responses. Neither the remaining 49% of visual neurons nor the remaining 67% of auditory neurons could have their responses classified as eye-centred or head-centred. In summary, it was found that both auditory and visual neurons had responses compatible with either eye-centred or head-centred frames of reference, although most neurons had complex responses that could not be classified into either of these categories. This was the first time that

head-centred neuronal responses were indentified in area LIP.   148

Previous Neural Network Models   149

[14] developed an early influemtial model that learned to transform an input   150
representation consisting of the position of the eye in the socket and the retinotopic   151
position of the visual target to an output representation consisting of the position of the   152
visual target with respect to the head. Specifically, two-dimensional representations of   153
the eye-position $\mathbf{e}$ and of the retinal location of the visual target $\mathbf{r}$ were used as input   154
for the neural network model. The target output used to guide the error-based update   155
of the synaptic weights during training was the head-centred location $\mathbf{h}$ of the visual   156
target represented by $\mathbf{r} + \mathbf{e}$. The model thus utilised a supervised, multi-layer   157
backpropagation of error network architecture, in which the output layer of the network   158
was provided with an explicit training signal representing the current head-centred   159
location of the visual target. Such a network architecture is not biologically plausible for   160
a couple of reasons. Firstly, it is not clear where such a training signal representing the   161
current head-centred location of the visual target might originate from in the brain.   162
Secondly, a multi-layer backropagation network architecture requires that the afferent   163
weights to the hidden layer be updated using an error signal based on the efferent   164
synaptic weights from these hidden neurons to the output layer scaled by the   165
corresponding errors in the output layer. Such a network architecture in itself is not   166
biologically plausible. Nevertheless, [14] found that training such a network to   167
transform independent eye position and retinal target position signals to head-centred   168
coordinates led to hidden units in the intermediate layer developing retinocentric   169
receptive fields with planar eye-position gain fields, very similar to those found in the   170
posterior parietal cortex by [6].   171

A number of later models that simulate the development of head-centred visual   172
neurons have also relied on some form of error correction learning. For example, the   173
model described by [15] relied on a form of supervised global error correction learning   174
that utilised an error term which is unlikely to be present in the cortex. The model of   175
sensorimotor transformation by [16] also used a supervised error correction learning rule   176
to modify the synaptic connectivity within the network. So, although supervised error   177
correction learning does not appear to offer a biologically plausible way of modelling the   178
development of head-centred visual neurons in the brain, it has nevertheless remained a   179
popular approach.   180

In contrast to the above error correction network models, [20] developed a model   181
that utilised associative learning. These authors investigated how retinotopic visual   182
representations could be transformed into head-centred representations that are relevant   183
to reaching tasks. It was hypothesised that the observation of our own motor   184
movements during a reaching task would be used to develop a map between the   185
eye-centred visual representation of the target and the head-centred motor   186
representation of the movement required to reach the target. In other words, the input   187
layer of the neural network model represented the visual signals generated by observing   188
the reaching movements, whilst the output layer represented the corresponding motor   189
movements that were performed. As with [14], the input representation consisted of the   190
position of the eye in the socket and the retinotopic position of the visual target, while   191
the output representation consisted of the head-centred target position. Hebbian   192
learning was then used during training to successfully associate each eye-centred visual   193
input representation of the target to the corresponding head-centred output motor   194
representation. In contrast to [14], the model developed by [20] did not use a   195
backpropagation of error network architecture or any other form of error correction.   196
Instead, they used a more biologically plausible associative learning rule to modify the   197
synaptic connectivity within their model. However, the model was still trained in a   198

supervised manner. That is, the network still made use of an explicit training signal in the output layer representing the head-centred location of the visual target in order to guide learning without an adequate explanation of where such a signal might originate from in the brain.

[22] proposed a hierarchical neural network model of coordinate transformation that used associative learning to set up the synaptic connectivity but did not require a biologically implausible supervisory training signal as used by [20]. The model developed by [22] had the following two main processing stages. The first processing stage used signals representing the retinotopic location of the visual target and signals representing the position of the eye to learn head-centred visual representations. The second processing stage used head position signals coupled with the head-centred visual representations developed by the first processing stage to learn body-centred visual representations. Training consisted of continously shifting a visual target presented to the network whilst randomly varying the position of the eyes and the head. Both processing stages used competitive learning with an associative learning rule to self-organise conjunctive representations of its respective inputs, and then used competitive learning with a form of temporally associative learning rule to bind representations that occurred close together in time. Learning in the second processing stage only started after the first processing stage had finished learning head-centred representations. This allowed each processing stage of the model to self-organise either head-centred or body-centred representations. Most importantly, in contrast to the models developed by [14] and [20], learning in [22] did not require the use of a biologically implausible supervisory training signal to guide learning of the coordinate transformations. However, the model of [22] did not investigate how the functional form of eye position gain modulation, i.e. monotonic *vs* peaked, may affect the development of head-centred visual representations. This is the focus of the current work presented below.

Our approach: A Biologically Plausible Unsupervised Self-organising Neural Network Model of Coordinate Transformation

Our laboratory has previously published a biologically plausible neural network model of the visually-guided development of head-centred visual neurons, which relies on associative learning rules and does not require a supervisory training signal to guide learning [1, 3]. Instead, our model utlises an unsupervised form of competitive learning that exploits the natural statistics of how primates move their eyes and head as they shift their gaze around their visual environment. Specifically, the model employs a form of *trace learning*, which encourages neurons in higher network layers to bind together input patterns that tend to occur close together in time. If a primate tends to move its eyes more frequently than adjusting the position of its head, then retinal images that occur close together in time will tend to correspond to different positions of the eyes but the same position of the head. In this case, trace learning will encourage neurons in higher layers to learn to respond to the position of a visual target in the same head-centred location across different retinal positions. Such neurons will have thus learned to represent the position of visual targets within a head-centred reference frame. The inputs to the model are eye-centred visual neurons that represent the locations of visual targets on the retina, but which have responses that are also gain modulated by the position of the eyes in the socket. In this paper, we investigate how the learning process depends on the functional form of this gain modulation by eye-position. Two forms of eye-position gain modulation are explored: monotonic gain modulation, which is dominant in most primate parietal areas (LIP, 7a, PRR), and peaked gain modulation

which is primarily found in area PO. ²⁴⁹

In the simulations described below in section Results, the model is found to robustly ²⁵⁰ develop head-centred output neurons with a standard trace learning rule when ²⁵¹ incorporating visual input neurons with *peaked* eye-position gain modulation [1], but not ²⁵² with *monotonic* eye-position gain modulation. Moreover, even if the model has its ²⁵³ synaptic connectivity perfectly prewired to perform a coordinate transformation from ²⁵⁴ eye-centred input neurons with monotonic gain modulation to head-centred output ²⁵⁵ neurons, subsequently introducing plasticity into the synaptic connections with the ²⁵⁶ standard trace learning rule quickly degrades the synaptic connectivity and eventually ²⁵⁷ leads to elimination of the head-centred output responses. Since eye-centred visual ²⁵⁸ neurons with monotonic eye-position gain modulation are so common in the dorsal ²⁵⁹ visual pathway [7, 23, 24], it is an important challenge to show how efferent synaptic ²⁶⁰ connections from these neurons may self-organise to produce head-centred visual ²⁶¹ responses in a subpopulation of postsynaptic receiving neurons. A subsequent analysis ²⁶² of the nature of the failure of the self-organisation of the synaptic connectivities led us ²⁶³ to explore the performance of the model with a variety of modified, yet still biologically ²⁶⁴ plausible, more powerful versions of the standard trace learning rule. The choice of the ²⁶⁵ modified versions of the trace learning rule used in this paper was motivated by the ²⁶⁶ superior performance of these learning rules reported by [25]. Here we show for the first ²⁶⁷ time how these modified learning rules enable the model to learn to perform a ²⁶⁸ coordinate transformation from eye-centred to head-centred reference frames even when ²⁶⁹ the visual input neurons have monotonic gain modulation by eye-position. ²⁷⁰

Materials and methods ²⁷¹

The Self-organisation of the Synaptic Connectivity within the ²⁷² Neural Network Model ²⁷³

The model uses four core components to self-organise head-centred visual ²⁷⁴ representations through a biologically plausible process of visually guided learning. The ²⁷⁵ first component is a population of input neurons that encode both the position of the ²⁷⁶ eyes in the orbit and the retinotopic location of visual targets. Such retinotopic visual ²⁷⁷ neurons with eye-position gain modulation have been identified in multiple primate ²⁷⁸ cortical areas [7–9, 23, 24]. The second component is a population of output neurons ²⁷⁹ that compete with each other through mutual inhibitory interactions, which is a ²⁸⁰ standard feature of cortical architecture [18]. The third component is a local synaptic ²⁸¹ *trace learning* rule to update the feedforward synaptic connections between the input ²⁸² and output neurons. The trace learning rule is a local associative learning rule that ²⁸³ incorporates an exponentially decaying temporal trace of past neuronal activity, and it ²⁸⁴ has been widely used in the context of developing invariant visual object ²⁸⁵ recognition [26, 27]. The trace learning rule has the effect of encouraging individual ²⁸⁶ postsynaptic neurons to learn to respond to subsets of input patterns that tend to occur ²⁸⁷ close together in time. Finally, the fourth component comes under the assumption that ²⁸⁸ visual stimuli are relatively static in a world reference frame during natural self-motion. ²⁸⁹ This assumption is justified by experimental findings in which primates adjust their ²⁹⁰ gaze more often by moving their eyes rather than the head itself [28]. This behavioural ²⁹¹ strategy to adjust gaze is preferable because it reduces the frequency of making more ²⁹² energetically costly and slow head movements. In fact, it has been found that during ²⁹³ exploration of natural environments with free head, eye and body movements, at any ²⁹⁴ time when there is movement, isolated head and isolated eye movements occurred 13.3% ²⁹⁵ and 33.1% of the time respectively, whilst a mixture of movements was observed in the ²⁹⁶ remaining time. That is, during natural movement there are periods when the eyes are ²⁹⁷

moving whilst the head remains stationary with respect to the visual environment and 298
visual objects also remain stationary within the environment. 299

These four model components allow the model to self-organise its synaptic 300
connectivity during visually guided training in the following way. If the eyes move 301
around a scene containing a stationary visual target while the head also remains 302
stationary, then the visual system will receive a sequence of input patterns with the 303
visual target in different retinal locations but the same head-centred location. That is, 304
the visual target remains stationary in the head-centred space, but changes its position 305
in the eye-centred space. The sequence of eye-positions and resulting retinal locations of 306
the visual target are represented by retinotopic visual input neurons with responses that 307
are gain modulated by eye-position. The synaptic trace learning rule is able to bind 308
subsets of input patterns corresponding to a visual target in the same head-centred 309
location, albeit with the visual target situated in different eye-centred locations, onto 310
the same output neurons. This is because input patterns corresponding to a visual 311
target situated in the same head-centred location tend to occur close together in time 312
due to the statistics of natural eye and head movements, in which the eyes tend to 313
saccade about a static visual scene while the head remains stationary. Moreover, the 314
naturally rapid movements of the eyes may expose the visual system to many such input 315
pattern sequences, where each such sequence has the visual target situated in the same 316
head-centered location but different randomised subsets of retinal locations. This 317
process will ensure that all possible input patterns corresponding to the same 318
head-centred location but different retinal locations are eventually brought into 319
temporal proximity with each other as training progresses. Hence, all input patterns 320
corresponding to the same head-centred location but different retinal locations would 321
tend to occur clustered together in time. This process continues with the visual target 322
seen in a different position within the head-centred space every time the position of the 323
head is shifted. That is, the natural head movements that occur between sequences of 324
rapid eye movements would shift the location of the visual target to new head-centred 325
locations. In this manner, the learning process is repeated with the visual target 326
presented in many different head-centred locations. New subsets of output cells would 327
learn to respond to the visual target in each different head-centred location due to the 328
competitive interactions between the output cells. Consequently, the output layer would 329
eventually develop neurons that cover the entire space of head-centred target locations. 330

The Architecture of the Self-Organising Neural Network Model   331

The neural network architecture of the model is shown in Fig 1. The network consists of 332
the following two layers of neurons. The first layer is a population of input neurons that 333
simultaneously encode the eye-position of the agent and the retinal location of the 334
visual target. These visual input neurons are modelled as retinotopic neurons with 335
eye-position gain modulation. The eye and retinal position spaces, representing the 336
range of eye-positions in orbit and retinal target locations, covered $[-30°, 30°]$ and 337
$[-90°, 90°]$, respectively. Feedforward synaptic connections project from neurons in the 338
input layer to neurons in the second layer. 339

Fig 1. Architecture of the neural network model. The competitive output layer
on the right receives afferent synaptic connections from neurons in the input layer on
the left. A trace learning rule is used to modify the strengths of the feedforward
synaptic connections from the input layer to the output layer during learning.

The second layer is a population of N output neurons that compete to represent 340
patterns in the input layer [18]. Neurons in the second layer, the *output layer*, all receive 341
the same number of afferent connections from neurons in the input layer, that is ϕ 342

percent of the input population, but each output neuron receives connections from its 343
own randomly assigned subset of the input neurons. Neither the output layer nor the 344
input layer is topographically organised. 345

The strengths of the feedforward synaptic connections from the input layer to the 346
output layer are initialised to random weights in the interval $[0, 1]$ at the start of each 347
simulation. The synaptic weight vector of each output neuron is then renormalised as is 348
typical in competitive networks [18]. 349

The Visually-Guided Training of the Network 350

The neural network is trained on input patterns that simultaneously encode both the 351
position of the eyes in orbit and the retinotopic position of the visual target. The 352
position of the eyes is kept within $[-24°, 24°]$, whilst the retinal locations of visual 353
targets are kept within the interval $[-63°, 63°]$. Keeping the position of the eyes and the 354
retinal locations of visual targets within these respective intervals reduces edge effects 355
due to clipping of the input representations. 356

Similarly, all M evenly spaced head-centred locations chosen for each experiment are 357
confined within $[-63°, 63°]$ to ensure that visual targets always remain in view as the 358
eyes move. Each training epoch consists of M periods, where each period individually 359
corresponds to one of the M chosen head-centred locations. During training, for each 360
period a visual target is fixed in a given head-centred location whilst the eyes perform a 361
series of saccades to P different and uniformly sampled eye-positions within $[-24°, 24°]$. 362
The saccades between successive eye-positions are performed at a constant velocity of 363
$400°/s$. The duration of each fixation is set to $300ms$. 364

Thus, the training process consisted of presenting to the network sequences of 365
combined visual and eye-position input signals, which represent the visual target in 366
fixed head-centred locations, whilst the eyes randomly shifted to different positions in 367
the orbit. 368

Testing the Network 369

The responses of the output units for all combinations of T head-centred visual target 370
locations and E eye fixation positions are recorded after training to test the model. In 371
order to test the ability of the trained model to generalise to new input patterns, the 372
model is tested with a set of novel combinations of eye-position and visual target 373
location not encountered during training. Specifically, the following $E = 4$ eye-positions 374
are used during testing: $-18°, -6°, 6°$ and $18°$. For each of these eye-positions, the 375
visual target is shifted in increments of $2°$ every $330ms$ to the next one of the $T = 80$ 376
head-centred target locations within $[-79°, 79°]$. The firing rates of all output neurons 377
are saved at the end of each fixation period to analyse the receptive field properties of 378
the neurons, including the receptive field size, receptive field location and reference 379
frame of response. 380

The Neuronal and Synaptic Dynamics of the Model 381

Input Layer 382

The firing rates of neurons in the input layer were modelled by a response function that 383
encodes the retinotopic location of a visual target, where the responses were modulated 384
by the position of the eyes in the orbit. The response function of each input neuron j 385
maps the current retinal location r of the visual target and the eye-position e onto the 386
neuron's instantaneous firing rate v_j^I. The instantaneous firing rate values are defined 387
within the range $[0, 1]$. We investigated the performance of the model when the response 388

functions of the input neurons were modulated by two different functional forms of eye   389
positon gain field as described next.   390

The first response function has a peaked eye-position gain field as shown in Fig 2**A**.   391
This form of eye-position modulation has been reported in cortical area PO by [9]. The   392
full response function is described by   393

$$v_j^I = \exp\left(-\frac{\|e - \beta_j\|^2}{2\rho^2}\right) \times \exp\left(-\frac{\|r - \alpha_j\|^2}{2\sigma^2}\right) \tag{1}$$

**Fig 2. Examples of the two alternative response functions used to compute
the firing rates of input neurons.** For each type of response function, we plot the
responses of an individual input neuron as a function of eye-position and retinal
location of a visual target. A: Example of a peaked response function, in which the
firing rate is modulated by a peaked eye-position gain field as described by Eq 1. B:
Example of a monotonic response function that is modulated by a sigmoidal
eye-position gain field described by Eq 2.

This response function is formed from a product of two components: the first   394
component represents the eye-position signal, whilst the second component encodes the   395
retinotopic position r of the visual target. In Eq 1, the neuronal response is modulated   396
by a peaked Gaussian function of eye-position. The parameter β_j denotes the preferred   397
eye-position for each input neuron j. The width of the corresponding Gaussian   398
eye-position tuning curve is determined by the standard deviation ρ. The preferred   399
retinal location of a target stimulus for each input neuron j is denoted by the parameter   400
α_j. The width of the corresponding Gaussian retinal tuning curve is determined by the   401
standard deviation σ. Each input neuron j is set to respond maximally to a unique   402
combination of retinal target location (α_j) and eye-position (β_j). The entire two   403
dimensional space consisting of possible combinations of eye-position and retinal target   404
location is covered by the population of input neurons in integer steps of 1 degree in   405
each dimension. This results in a total of $201 \times 61 = 12,261$ neurons in the input layer.   406
The second form of firing rate response function used to model the input neurons   407
incorporates a sigmoid eye-position gain field as shown in Fig 2**B**. This form of   408
eye-position modulation is monotonic in the eye-position dimension, as has been   409
observed in multiple visual areas [7,8]. Although the form of the modulation is   410
sigmoidal whilst most empirical work has described it as planar, [16] showed the data is   411
also compatible with a saturating sigmoidal gain formulation. The full response   412
function is described by   413

$$v_j^I = \frac{1}{1 + \exp\left(\kappa_j(e - \beta_j)\right)} \times \exp\left(-\frac{\|r - \alpha_j\|^2}{2\sigma^2}\right) \tag{2}$$

In Eq 2, the visual receptive field is modulated by a sigmoidal function of   414
eye-position. For each input neuron j, the parameter κ_j determines the gain direction   415
and saturation rate of the modulation, where κ_j is $-2\times$ the slope of the sigmoid. The   416
inflection point β_j determines the eye-position where a firing rate response greater than   417
0.5 begins. The input neurons all have the same absolute saturation rate, that is   418
$|\kappa_j| = |\kappa_m|$ for all j and m, but one half has a positive gain direction ($\kappa_j > 0$) whilst   419
the other half has a negative gain direction ($\kappa_j < 0$). Each input neuron j is set to   420
respond maximally to a unique combination of retinal target location α_j, eye-position   421
β_j, and gain direction and saturation rate κ_j. The population of input neurons evenly   422
covers the entire three dimensional space resulting from such combinations. This results   423
in an input population of $201 \times 61 \times 2 = 24,522$ neurons.   424

Output Layer

Three dynamical quantities were defined for each neuron i in the competitive output layer: an internal activation $h_i(t)$, a memory trace value $q_i(t)$, and an instantaneous firing rate $v_i(t)$ [29].

The internal activation is governed by the equation

$$\tau_h \frac{dh_i}{dt} = -h_i + \sum_j w_{ij} v_j^I \tag{3}$$

where w_{ij} denotes the strength of the synapse from the jth input neuron to the ith output neuron and τ_h is a time constant common for all output neurons.

The instantaneous firing rate is given by

$$v_i^I = \frac{1}{1 + \exp\left(-2\varphi(h_i - p_\pi - \theta)\right)} \tag{4}$$

where θ and φ denote the sigmoid threshold and slope, respectively. The level of competition between neurons in the output layer, and thereby the proportion of neurons that remained active, is controlled by the parameter p_π. Specifically, the parameter p_π is set to the πth percentile point of the distribution of neuronal activations within the output population. For example, p_π is set to the top tenth percentile activation value when π is set to 90. This way of implementing competition within the competitive output layer has been previously used in competitive neural network models of the primate visual system with trace learning [30]. In the cortex, lateral inhibition is implemented via inhibitory interneurons [29]. The trace value $q_i(t)$ is defined in the following section.

Modification of Synaptic Weights by Trace Learning

Trace learning rules for synaptic modification encourage postsynaptic (output) neurons to bind together subsets of input patterns that tend to occur close together in time by incorporating a temporal trace of recent neuronal activity. The trace value $q_i(t)$ for the ith neuron in the output layer is given by

$$\tau_q \frac{dq_i}{dt} = -q_i + v_i \tag{5}$$

where v_i is the instantaneous firing rate of the neuron, and τ_q is a time constant common for all output neurons.

In the first part of the paper, during training the strength of the synapse from the jth input neuron to the ith output neuron is governed by the standard trace learning rule previously implemented by [1]

$$\frac{dw_{ij}}{dt} = \varrho q_i v_j^I \tag{6}$$

where ϱ is the learning rate, v_j^I is the instantaneous firing rate of the jth input neuron and q_i is the trace value of the ith output neuron. However, later in this paper we will introduce a number of new, more powerful forms of trace learning, which are in fact needed to produce head-centred output neurons when the input neurons are modulated by a sigmoidal (monotonic) function of eye-position.

Finally, after each weight update during training, the length of the weight vector for each output neuron i, that is $\mathbf{w}_i = (w_{i1}, \ldots, w_{iN_I})$ where there are N_I input neurons, is renormalised by setting

$$\mathbf{w}_i := \frac{\mathbf{w}_i}{\|\mathbf{w}_i\|} \tag{7}$$

This prevents unbounded growth of the synaptic weights during training [29]. Experimental evidence for renormalisation of synaptic weights in the brain has been reported by [31].

Simulation of the Differential Model

The Forward-Euler scheme is used to numerically integrate the coupled differential equations given by Eq 3 and Eq 5-6. The numerical time step Δt is set to one tenth of the neuronal time constant τ_h. We checked that the simulation results remained similar if the time step was reduced or the number of training epochs increased.

During training and testing, the input patterns encoding the changing eye-position and retinotopic target location are simulated dynamically and sampled at 1kHz. Linear interpolation is used to compute the numerical inputs to the discretised Forward Euler model equations, which require input values at every numerical time step $\Delta t = \tau_h/10$.

Analysis of Network Performance

In order to analyse whether individual output neurons are predominantly responding in an eye-centred or head-centred frame of reference, we used a method of analysis originally developed by [1]. This analysis is described next with the mathematical details taken from that earlier paper.

Let $\mathbf{R}$ be a matrix containing the responses of a given neuron during testing, where $\mathbf{R}[i,j]$ denotes the firing rate when the model is fixating in the ith eye-position e_i and the visual target is in the jth head-centred location t_j, as recorded during the testing protocol described above. The vector $(\mathbf{R}[i,1],\ldots,\mathbf{R}[i,T])$ is referred to as the response vector at the ith eye-position. The number of eye-positions during testing is denoted by E, while the number of head-centred locations for visual targets during testing is denoted by T. The indexing of eye-positions and head-centred target locations are ordered from left (negative) to right (positive), that is $e_1 \leq \ldots \leq e_E$ and $t_1 \leq \ldots \leq t_T$.

To determine which reference frame an output neuron is responding in during testing, two separate metrics are applied that reflected to what degree the neuronal response is compatible with either an eye-centred or head-centred reference frame, and then the values of these two metrics are compared.

The head-centredness metric computed the degree to which the head-centred response vectors of a neuron remained stable across different eye-positions. The head-centredness metric measured the degree of such stability for a given output neuron by averaging correlations between response vectors for different eye-positions, that is

$$\Pi = \frac{1}{\binom{E}{2}} \sum_{1 \leq i_1 < i_2 \leq E} \frac{\sum_{j=1}^{T} \left(\mathbf{R}[i_1,j] - \overline{\mathbf{R}}[i_1]\right)\left(\mathbf{R}[i_2,j] - \overline{\mathbf{R}}[i_2]\right)}{\sqrt{\sum_{j=1}^{T} \left(\mathbf{R}[i_1,j] - \overline{\mathbf{R}}[i_1]\right)^2 \sum_{j=1}^{T} \left(\mathbf{R}[i_2,j] - \overline{\mathbf{R}}[i_2]\right)^2}} \tag{8}$$

where

$$\overline{\mathbf{R}}[i] = \frac{1}{T} \sum_{j=1}^{T} \mathbf{R}[i,j] \tag{9}$$

This yielded a metric which is referred to as the *head-centredness* of the output neuron, and it is bounded between -1 and 1, where a perfect correlation of 1 indicated a perfectly head-centred response.

A very similar analysis is done to quantify the compatibility of the responses of the output neuron with an eye-centred frame of reference. That is, a visual neuron is judged

to respond in an eye-centred frame of reference to the extent that its eye-centred response vectors remain stable across different eye-positions. The eye-centred analysis proceeded as follows. To reiterate, each response vector $(\mathbf{R}[i, 1], \ldots, \mathbf{R}[i, T])$ is the result of testing over the same set of head-centred locations, but with the model fixated in a distinct eye-position. Therefore, each response vector also corresponded to a unique range of retinal locations. The *intersection* of these retinal ranges corresponded to different portions of each response vector, and it is these portions that are subject to correlation analysis. Specifically, f_i denotes the first vector position in the ith response vector to be included, and the $V - 1$ next positions are included as well such that the subvector $(\mathbf{R}[i, f_i], \ldots, \mathbf{R}[i, f_i + (V - 1)])$ is the vector being used for the correlation analysis. The derivation of f_i and V are found in the appendix Appendix A. This gave the metric

$$
\Omega = \frac{1}{\binom{E}{2}} \sum_{1 \leq i_1 < i_2 \leq E} \frac{\sum_{j=0}^{V-1} \left(\mathbf{R}[i_1, f_{i_1} + j] - \overline{\mathbf{R}}[i_1]\right) \left(\mathbf{R}[i_2, f_{i_2} + j] - \overline{\mathbf{R}}[i_2]\right)}{\sqrt{\sum_{j=0}^{V-1} \left(\mathbf{R}[i_1, f_{i_1} + j] - \overline{\mathbf{R}}[i_1]\right)^2 \sum_{j=0}^{V-1} \left(\mathbf{R}[i_2, f_{i_2} + j] - \overline{\mathbf{R}}[i_2]\right)^2}} \tag{10}
$$

where

$$
\overline{\mathbf{R}}[i] = \frac{1}{V} \sum_{j=0}^{V-1} \mathbf{R}[i, f_i + j] \tag{11}
$$

This is referred to as the *eye-centredness* of the output neuron, and it is bounded between -1 and 1, where a perfect correlation of 1 indicated a perfectly eye-centred response. Response vectors which had no response for the extracted ranges are excluded from the correlation, and a neuron without a response within this range of retinal locations at any eye-position is excluded from further analysis.

A neuron is finally classified as head-centred if $\Pi > 0$ and $\Pi > \Omega$, and classified as eye-centred if $\Omega > 0$ and $\Omega > \Pi$. If neither of these conditions is met then the neuron remains unclassified.

Results

Self-organisation with peaked and monotonic gain fields

This experiment explores the feasibility of the self-organisation of head-centred receptive fields under the two different forms of eye-position gain modulation. Two models are trained and tested on the same stimuli, where one model has peaked eye-position modulation in the input population as shown in Fig 2**A**, and the other model has sigmoidal modulation as shown in Fig 2**B**. The training lasts for 20 epochs. During each training epoch, a visual target is presented for approximately $5s$ in each of the eight head-centred training locations: $-63°, -45°, -27°, -9°, 9°, 27°, 45°$ and $63°$. For each period where the visual target is in a fixed head-centred target location, the eye-position is varied continuously through time as the model makes a series of saccades and fixations. During each such period, the model performs 14 saccades interleaved with 15 fixations, where each fixation lasts $300ms$. Each saccade is at a constant velocity of $400°/s$, and it is directed to a random eye-position within the range $[-24°, 24°]$. Each training epoch thus lasts for approximately $40s$, and the entire training of the network is completed after about $800s$ of simulated time. The model is tested as previously described. The parameters for the two model simulations are given in Table 1.

Fig 3 compares the firing rate responses of the output neurons before and after training in the two models with either peaked or sigmoidal gain modulation of the

Table 1. Simulation parameter of self-organising models with either peaked or sigmoidal eye-position gain modulation.

Parameter	Symbol	Value (peaked)	Value (sigmoid)
Number of target locations	M	8	8
Fixation sequence length	P	15	15
Number of training epochs	-	20	20
Width of peaked eye-position tuning curve	ρ	6°	-
Width of retinal tuning curve	σ	6°	6°
Gain magnitude	$|\kappa|$	-	0.0625
Output neuron population size	N	900	900
Input neuron population size	N_I	12261	24522
Trace time constant	τ_q	400ms	400ms
Activation time constant	τ_h	100ms	100ms
Activation function slope	φ	4.5	4.5
Activation function threshold	θ	0.4	0
Sparseness percentile	π	80%	90%
Learning rate	ϱ	0.05	0.05
Synaptic connectivity	ϕ	5%	5%

visual input neurons. The responses of an output neuron from the model with peaked eye-position gain modulation before training (Fig 3**A**) exhibits no consistent structure in head-centred space across the different eye-positions. However, after training (Fig 3**B**) there is a clear maximal response to the same head-centred location across all eye-positions. Therefore, the self-organisation process has made the response reference frame of this output neuron strongly head-centred. The responses of an output neuron from the model with sigmoidal eye-position gain modulation before training (Fig 3**C**) also has an erratic and more eye-centred response prior to training due to the randomly assigned synaptic weights. However, unlike the peaked gain modulation model, training has the effect of making the neuron almost perfectly eye-centred. This is clearly seen by the receptive fields shifting in head-centred space in register with the eye-position shifts. Therefore, the self-organisation process has made this output neuron even more compatible with an eye-centred reference frame. The miniature scatter plots show the reference frame values of all neurons in the output layer, where each neuron is plotted as a point corresponding to that neuron's particular combination of head-centredness and eye-centredness. The miniature scatter plots confirm the same general effects across the entire populations of output neurons. That is, subplot (**B**) shows that a large proportion of the output neurons in the model with peaked gain modulation have a high head-centredness and low eye-centredness, and thus respond in a head-centred reference frame. While subplot (**D**) shows that a large proportion of the output neurons in the model with sigmoidal gain modulation have a low head-centredness and high eye-centredness, and thus respond in an eye-centred reference frame.

Fig 4 shows the synaptic weight vectors of the same output neurons as those shown in Fig 3. Before training, there is no structure to the potentiated synapses of the output neurons in terms of the preferences of the presynaptic input neurons (Fig 4**A** and Fig 4**C**), reflecting the random weighting assigned to an untrained network. After training, the synaptic weight vector of the output neuron from the model with peaked eye-position gain modulation shows a clear diagonal structure (Fig 4**B**). This synaptic weight profile is consistent with a learned response to a particular location within the head-centred frame of reference, and is thus consistent with the observed head-centred responses of this neuron during testing (Fig 3**B**). The synaptic weight vector of the

Fig 3. Comparison of model performance with peaked and sigmoidal (monotonic) gain modulation of visual input neurons. The figure shows the firing rate responses of output neurons before and after training with the standard trace rule (6). Specifically, each subplot shows the firing rate responses of a typical output neuron during testing for four different eye-positions: $-18°, -6°, 6°$ and $18°$. The top row shows output neuron #95 from the model with peaked eye-position gain modulation before training **(A)** and after training **(B)**. The bottom row shows output neuron #838 from the model with sigmoidal eye-position modulation before training **(C)** and after training **(D)**. In each subplot, each curve corresponds to a fixed eye-position while a visual target is presented across the same range of head-centred locations. It is evident in subplot **(B)** that after training the model with peaked gain modulation of the input neurons, the output neuron responds reasonably consistently when the visual target is presented within the localised interval of head-centred space $[0°, 16°]$ regardless of the eye-position. The neuron is thus responding in a head-centred reference frame. However, in contrast, subplot **(D)** shows that after training the model with sigmoidal (monotonic) gain modulation, the responses of the output neuron in the head-centred visual space are much more dependent on the eye-position. Thus, this neuron is not representing the target position in a head-centred reference frame. The miniature scatter plots show the reference frame values of all neurons in the output layer, where each neuron is plotted as a point corresponding to that neuron's particular combination of head-centredness (ordinate) and eye-centredness (abscissa). The neuron whose firing rate responses have been plotted is shown in the scatter plot by a red mark. The miniature scatter plots confirm the same general effects across the entire populations of output neurons. That is, subplot **(B)** shows that a large proportion of the output neurons are clustered in the top left quadrant of the scatter plot, indicating a high head-centredness (ordinate) and low eye-centredness (abscissa). These output neurons are thus responding in a head-centred frame of reference. While subplot **(D)** shows that a large proportion of the output neurons are clustered in the bottom right quadrant of the scatter plot, indicating a low head-centredness (ordinate) and high eye-centredness (abscissa). Thus, with monotonic gain fields acting on the input neurons, the population of output neurons have overwhelmingly learned to respond in an eye-centred reference frame.

neuron from the model with sigmoidal (monotonic) gain modulation exhibites an entirely different pattern of potentiation after training. In this case, the strenghtened synapses have an approximately horizontal structure that is concentrated on input neurons corresponding to a small portion of retinal preference space (Fig 4**D**). As a result, this output neuron has learned an eye-centred response (Fig 3**D**).

Fig 5 shows the reference frame values for all output neurons from both models with either peaked or sigmoidal gain modulation tested before and after training. It is clear that, for the model with peaked eye-position modulation, training has the effect of making the majority of output neurons head-centred, and also with a much larger head-centredness value. Specifically, before training 26% of output neurons are head-centred, and after training 69% are head-centred. Moreover, among the head-centred neurons, the average head-centredness rose from 0.17 before training to 0.63 after training. For the model with sigmoidal eye-position modulation, training has the effect of keeping the majority of output neurons eye-centred, and indeed increasing their average eye-centredness from 0.88 to 0.96.

In summary, when the visual input neurons have peaked eye positon gain modulation, training the network has the effect of developing head-centred output neurons. However, when the input neurons have sigmoidal (monotonic) gain modulation, the training process makes most output neurons almost perfectly eye-centred.

Since a large proportion of visual neurons in the dorsal visual pathway have

Fig 4. Strengths of the afferent synapses from the input population to a typical output neuron during testing. Results are shown for the model with peaked eye-position gain modulation before training (**A**) and after training (**B**), and for the model with sigmoidal eye-position modulation before training (**C**) and after training (**D**). The output neurons correspond to those plotted in Fig 3. In each plot, the afferent synapses have been arranged topographically by the preference of the input neuron for retinal location α_i and eye-position β_j. For the model with sigmoidal gain modulation, there are two input neurons for every combination of retinal preference and eye-position preference, but with opposite eye-position gain. Consequently, the input population has been separated by gain direction. The portion of each plot to the left of the white dashed line corresponds to input neurons with positive gain $\kappa_j > 0$, while the portion of each plot to the right of the white dashed line corresponds to those input neurons with negative gain $\kappa_j < 0$. It can be seen from subplot (**B**) that the output neuron in the trained network with peaked gain modulation has developed a diagonal weight structure, which is consistent with a learned response to a particular location within the head-centred frame of reference. In contrast, subplot (**D**) shows that the output neuron in the trained network with sigmoidal (monotonic) gain modulation has developed a more horizontal weight structure, which is consistent with a learned response to a specific location within the eye-centred reference frame.

Fig 5. Scatter plot of eye-centredness and head-centredness values of output neurons from simulations with peaked and monotonic gain modulation. The scatter plot shows the eye-centredness and head-centredness values of all output neurons from four separate simulations corresponding to the models with peaked and sigmoidal (monotonic) gain modulation tested before and after training with the standard trace rule (Eq 6). Each point in the scatter plot corresponds to an output neuron from the given simulation, plotted in terms of its eye-centredness (abscissa) and head-centredness (ordinate). The dashed diagonal line with positive unity slope separates those neurons which are classified as head-centred (above line) from those that are classified as eye-centred (below the line). It is evident that after training most of the output neurons from the network with peaked gain modulation have become head-centred, while nearly all of the output neurons from the network with monotonic gain modulation have remained eye-centred.

responses that are modulated by a monotonic function of eye-position, it is important to understand why monotonic gain fields make it more difficult for trace learning to produce head-centred output neurons. In the next section, we investigate this problem by carrying out a covariance analysis on the input patterns themselves.

Covariance Analysis of the Effects of Gain Modulation

The preceeding model simulations failed to develop head-centred output representations during self-organisation when the input population had sigmoidal eye-position modulation, despite succeeding with peaked eye-position modulation. This raises the question of what the difference is between the two different forms of input encoding from the perspective of competitive learning [18]. It is well known that standard competitive networks develop weight vectors that reflect the covariance between the activities of input neurons. In particular, there is a tendency for output neurons to learn to respond to subsets of input neurons whose activities are highly correlated. Hence inspecting the covariance between input neurons across all input patterns may reveal what structure the weight vectors should converge towards under standard competitive learning conditions with a Hebbian learning rule.

The covariance between input neurons may be computed in the same way for both input neurons with peaked gain described by Eq 1 and input neurons with sigmoidal gain described by Eq 2. In the case of an input neuron with retinal preference α and eye-position preference β, the covariance between it and a second input neuron with corresponding preferences α^*, β^* is given by

$$\text{cov}_{\alpha,\beta}(\alpha^*, \beta^*) = \iint\limits_{R \times E} \left(R_{\alpha,\beta}(r,e) - \overline{R}_{\alpha,\beta} \right) \left(R_{\alpha^*,\beta^*}(r,e) - \overline{R}_{\alpha^*,\beta^*} \right) dr de \qquad (12)$$

$R_{\alpha,\beta}(r,e)$ is the response of a neuron with preferences α, β to a visual target at retinal location r and eye-position e, as given by either Eq 1 or Eq 2. The term $\overline{R}_{\alpha,\beta}$ is the average response of the same neuron across all possible inputs in the $R \times E$ space, that is

$$\overline{R}_{\alpha,\beta} = \frac{1}{|R \times E|} \iint\limits_{R \times E} R_{\alpha,\beta}(r,e) dr de \qquad (13)$$

Fig 6**A** shows this covariance map for an input neuron with a peaked gain and preferences $\alpha = \beta = 0°$, and Fig 6**B** shows the covariance map for an input neuron with sigmoidal gain and preferences $\alpha = \beta = 0°$ and $\kappa > 0$.

Fig 6. Covariance between a given input neuron and the rest of the input neuron population. Each plot shows the covariance between a given input neuron and the rest of the input neuron population in the form of a topographic map analogous to the weight vector maps shown above. Subplots **(A)** and **(B)** show results for input neurons with peaked and monotonic gain, respectively. In both cases the input neuron has preferences $\alpha = \beta = 0°$, and in the monotonic case the input has positive gain ($\kappa > 0$).

The structure of covariance in the peaked modulation case is functionally identical to the response function of the input neuron, namely a two dimensional Gaussian tuning curve. The form of this covariance function is obvious by considering the correlations between the activities of input neurons with peaked gain.

In the sigmoidal (monotonic) modulation case, the situation is more complicated. The strong covariance is localised within the retinal preference dimension, but elongated within the eye-position dimension. This can again be understood by considering the response functions of the input neurons. Firstly, because all input neurons have a sharp, peaked tuning profile in the retinal preference dimension, any two input neurons need to have similar retinal preferences in order to have the possibility of being coactive. This explains the localisation of strong covariance in the retinal preference dimension. Secondly, the elongated form of the covariance function in the eye-position dimension results directly from the sigmoidal gain as follows. In the subpopulation of input neurons with a positive gain direction, similar to the reference input neuron $(0°, 0°)$ itself, it is clear that other neurons with a similar retinal preference and with an eye-position preference to the right (i.e. larger than $0°$) cofire more frequently with the reference neuron. This is because a positive gain implies that an input neuron responds to all eye-positions to the left of (i.e. smaller than) the eye-position preference of the neuron. Conversley, a negative gain implies that an input neuron responds to eye-positions to the right of (i.e. greater than) the eye-position preference of the neuron. Hence, in the subpopulation of input neurons with a negative gain direction, it can be seen that neurons with a similar retinal preference and with an eye-position preference to the left of (i.e. smaller than) $0°$ cofire more frequently with the reference neuron.

The covariance maps shown in Fig 6**A** and Fig 6**B** predict the structure of the weight vectors that we would expect to see develop in a competitive network with a standard

Hebbian learning rule trained over all input patterns with either peaked or sigmoidal ^{643} gain, respectively. These predictions are tested by running simulations with a Hebbian ^{644} learning rule with both peaked and sigmoidal gain modulated input neurons. The ^{645} Hebbian learning rule is implemented in the model by replacing the trace value q_i in the ^{646} standard trace learning rule (Eq 6) by the current firing rate v_i of the postsynaptic ^{647} neuron. For each simulation, there are 200 training patterns corresponding to random ^{648} locations in the $E \times R$ space. The activation time constant is reduced to $\tau_h = 30ms$ to ^{649} avoid any trace effect during learning. Fig 7**A** and Fig 7**C** show the synaptic weight ^{650} vectors of two typical output neurons that developed after training with the Hebbian ^{651} learning rule when the input neurons are modulated by either peaked or monotonic gain, ^{652} respectively. It is clear that these synaptic weight vectors have a very similar structure ^{653} to the corresponding covariance maps shown in Fig 6. Thus, with the Hebbian learning ^{654} rule, the underlying correlations between the activities of the input neurons with either ^{655} peaked or sigmoidal gain shape the synaptic weight structure that develops during ^{656} training. Most importantly, with monotonic gain, the synaptic weights are localised ^{657} within the retinal preference dimension, but elongated within the eye-position preference ^{658} dimension. This kind of synaptic weight structure leads to eye-centred output responses. ^{659}

Fig 7. Weight vectors of two typical output neurons. The top row shows the weight vectors of two typical output neurons that develop when the input neurons have peaked eye-position gain modulation and the network is trained with either the Hebbian learning rule **(A)** or the trace learning rule **(B)**. The bottom row shows the weight vectors of two typical output neurons when the input neurons have monotonic eye-position gain and the network is trained with either the Hebbian learning rule **(C)** or the standard trace learning rule **(D)**.

Next, comparison simulations are run with the trace learning rule. Fig 7**B** and ^{660} Fig 7**D** show the synaptic weight vectors of two typical output neurons that developed ^{661} after training with the trace learning rule when the input neurons are modulated by ^{662} either peaked or sigmoidal gain, respectively. Fig 7**B** shows a diagonal band of ^{663} potentiated synaptic weights, which correspond to input neurons representing the same ^{664} head-centred location but with different combinations of retinal location and ^{665} eye-position. Thus, with peaked gain, the trace learning rule is able to simply bind ^{666} together clusters of input neurons along a diagonal line in the (retinotopic preference $\times$ ^{667} eye-position preference) input space corresponding to a particular head-centred location. ^{668} Output neurons will then respond to particular head-centred locations regardless of ^{669} eye-position or the retinal location of a visual target. However, the situation is quite ^{670} different with sigmoidal gain modulated input neurons. Fig 7**D** shows a similar ^{671} horizontal weight structure to that obtained with the Hebbian learning rule (Fig 7**C**). ^{672} In particular, in both of these last two cases, the weight vector is very similar to the ^{673} covariance structure found among the input neurons with sigmoidal eye-position ^{674} modulation (Fig 6**B**). Thus, with sigmoidal gain, even if a trace learning rule is ^{675} implemented, the output neurons still learn to represent eye-centred rather than ^{676} head-centred locations. This is because developing head-centred output responses would ^{677} require the trace learning rule to do more than simply bind input patterns together. ^{678} With sigmoidal gain, trace learning must also disrupt and break apart output ^{679} representations corresponding to clusters of highly correlated input neurons, which are ^{680} localised in the retinotopic preference dimension but elongated in the eye-position ^{681} preference dimension. However, in practice the standard trace learning rule given by ^{682} Eq (6) is not strong enough to achieve this. Consequently, with the standard trace ^{683} learning rule, these elongated clusters of input neurons with correlated activities ^{684} continue to drive the development of eye-centred output neurons, as observed in the ^{685} simulations previously reported in this article (section Self-organisation with peaked and ^{686}

monotonic gain fields).   687

Introducing Plasticity into a Prewired Model   688

The failure of self-organisation to produce head-centred output neurons in a model with   689
sigmoidal (monotonic) eye-position gain modulation suggests the following two   690
important questions. First, does there actually exist a synaptic weight connectivity   691
matrix that would support a mapping to head-centred output representations, even if in   692
practice the self-organisation process using the standard trace learning rule (6)   693
originally implemented by [1] fails to converge on this solution? Secondly, if it is   694
possible to prewire a network with such a synaptic weight structure, then would the   695
head-centred output representations be abolished by subsequently introducing synaptic   696
plasticity either in the form of the standard trace learning rule (6) or normal Hebbian   697
learning (where the trace value q_i is replaced by the current firing rate v_i)? If so, then   698
this would demonstrate an even deeper problem: the presence of such forms of synaptic   699
plasticity in a network with sigmoidal gain modulation not only fails to drive the   700
development of head-centred output representations, but would also abolish any existing   701
head-centred representations.   702

To address the above two questions, we construct a manually prewired model that is   703
designed to produce head-centred output neurons with input neurons that are   704
modulated by sigmoidal functions of eye-position. The prewired model is constructed as   705
follows. There are 24522 neurons in the input population, each corresponding to a   706
unique combination of retinal-position preference (α_i), eye-position preference (β_j) and   707
slope (κ_j). There are 900 neurons in the output population, each given a head-centred   708
receptive field at one among nine head-centred locations, which are $-68°$, $-51°$, $-34°$,   709
$-17°$, $0°$, $17°$, $34°$, $51°$ and $68°$. Each neuron in the output population is   710
postsynaptically connected to a randomly assigned subpopulation of the input   711
population. There are only two synaptic weight values across all synapses, simply   712
referred to as elevated and depressed. The strength of a synapse is elevated if the   713
presynaptic input neuron responded maximally to a combination of eye-position and   714
retinal location corresponding to a head-centred location that is closest to the   715
head-centred location assigned to the output neuron. Otherwise the synapse is   716
depressed. Therefore, the output neuron receives strong driving input to the extent that   717
a visual target is near its assigned head-centred location. Specifically, the weight of a   718
synapse with a postsynaptic neuron assigned to head-centred receptive field location h 719
and a presynaptic neuron having retinal-preference α, eye-position preference β and   720
$\kappa > 0$ is given by   721

$$w_{h,\alpha,\beta} = \begin{cases} 10 & h - \beta \leq \alpha \leq h + W/2 \quad \text{(Elevated)} \\ 1 & \text{else} \qquad\qquad\qquad\quad \text{(Depressed)} \end{cases} \tag{14}$$

where $W = 60°$ is the size of the eye-position dimension. Likewise when $\kappa < 0$ the   722
weight is given by   723

$$w_{h,\alpha,\beta} = \begin{cases} 10 & h - W/2 \leq \alpha \leq h - \beta \quad \text{(Elevated)} \\ 1 & \text{else} \qquad\qquad\qquad\quad \text{(Depressed)} \end{cases} \tag{15}$$

Fig 8 shows the structure of the canonical weight vector produced by Eq 14-15.   724
Before testing the network, the synaptic weight vectors of all output neurons underwent   725
the normalization step described by Eq 7. To provide a baseline for comparison, a   726
network with randomly wired synaptic connections is also tested in the same way. The   727
parameters for both models are given in Table 2.   728

Fig 9 shows the eye-centredness and head-centredness values of output neurons in   729
the manually prewired model as well as a randomly wired model for comparison. It is   730

Fig 8. Synaptic weight structure of a network model that has been manually prewired in order to produce head-centred output neurons with input neurons that are modulated by a sigmoidal function of eye-position. The figure shows the structure of the canonical weight vector resulting from the prewiring Eq 14 and Eq 15. Each of the two rectangles represents the topographic organisation of one half of the input population in terms of retinal-preference (α_i) and eye-position preference (β_j), with the input neurons in the left rectangle having $\kappa > 0$ (positive gain) and the right rectangle having $\kappa < 0$ (negative gain). A neuron in the competitive output population which has been assigned a head-centred receptive field at location h will have elevated connections from input neurons with preferences located in the right-angled triangles of the input space, labeled **A** and **B**.

Table 2. Simulation parameters of the network model that has been manually prewired in order to produce head-centred output neurons with monotonic modulated input neurons.

Parameter	Symbol	Value
Width of retinal tuning curve	σ	$6°$
Gain magnitude	$|\kappa|$	0.0625
Output neuron population size	N	900
Input neuron population size	N_I	24522
Activation time constant	τ_h	100ms
Activation function slope	φ	4
Activation function threshold	θ	0
Sparseness percentile	π	90%
Synaptic connectivity	ϕ	8.16%

clear that in the manually prewired model, the majority of output neurons are   731
head-centred. In contrast, there are no head-centred neurons in the randomly wired   732
model. In summary, the results from the manually prewired model demonstrate the   733
existence of a synaptic weight matrix which allows the output neurons to perform the   734
desired coordinate transformation to a head-centred reference frame even when the   735
input neurons are modulated by a sigmoidal function of eye-position.   736

Fig 9. Performance of the prewired network model with monotonic modulated input neurons. The Figure shows the performance of the network model that has been manually prewired to produce head-centred output neurons with input neurons that are modulated by a sigmoidal function of eye-position. The scatter plot shows the eye-centredness and head-centredness values of all output neurons from the manually prewired model and a randomly wired model. Same conventions as in Fig 5. It can be seen that the majority of the output neurons in the manually prewired model display head-centred responses.

The next question to be explored is, what would be the effect of introducing   737
synaptic plasticity, either in the form of the standard trace learning rule (6) or normal   738
Hebbian learning, into the manually prewired model while it is exposed to the kinds of   739
visual input described above? This experiment would inform whether these forms of   740
plasticity not only failed to drive the development of head-centred output   741
representations during self-organisation, but would even abolish existing head-centred   742
representations. The manually prewired model is therefore subjected to the same visual   743
training stimuli as described above over 10 training epochs. The results presented here   744
are from a simulation using the standard trace learning rule (6). However, although not   745

shown, further simulations with a Hebbian learning rule without an explicit memory   746
trace gave qualitatively similar results.   747

The impact of introducing synaptic plasticity into the manually prewired modelsas is   748
inspected by plotting key summary statistics as a function of the number of training   749
epochs in Fig 10. There is a catastrophic drop in model performance after only the first   750
epoch of training, where the fraction of head-centred neurons decreased from ∼77% to   751
∼0.3%, and the average head-centredness among head-centred neurons decreased from   752
∼0.7 to ∼0.26. Subsequent training epochs remained around these levels. After epoch 5   753
there is not a single head-centred neuron.   754

**Fig 10. The effects of introducing synaptic plasticity into the network that
has been manually prewired to produce head-centred output neurons when
the input neurons that are modulated by a sigmoidal (monotonic) function
of eye-position.** The figure shows population analyses of the response properties of
output neurons in the manually prewired model as the synaptic weights are further
modified during ten training epochs with the standard trace learning rule (6). Three
key summary statistics are given. The head-centredness rate (red) is the fraction of
head-centred neurons in the output population. The average head-centredness (green) is
the average head-centredness among head-centred neurons, and becomes undefined if no
head-centred neurons are found to exist. The average eye-centredness (blue) is the
average eye-centredness among all output neurons. The dashed lines show these values
for the manually prewired network before training, while the unbroken lines show the
values through successive training epochs after synaptic plasticity has been introduced.
The error bars are the standard deviations. It can be seen that by the end of the first
training epoch the majority of the output neurons switched from being head-centred to
eye-centred.

In summary, it is found that just a single training epoch switched most of the output   755
neurons from being head-centred to eye-centred. We hypothesised that this is due to the   756
same visually-guided learning dynamics described above in section Self-organisation   757
with peaked and monotonic gain fields and in section Covariance Analysis of the Effects   758
of Gain Modulation, which come into operation when the retinotopic input neurons   759
have monotonic eye-position gain modulation. Thus, even if the synaptic weights are   760
initially manually prewired to effect head-centred output responses, which might be   761
suggested to happen in the brain through genetic specification, the introduction of just   762
a limited amount of synaptic plasticity, either in the form of the standard trace learning   763
rule (6) or normal Hebbian learning, and visually-guided learning led to the output   764
neurons rapidly switching to eye-centred responses. The presence of even modest levels   765
of such synaptic plasticity will quickly overwrite head-centred representations that have   766
been set up through structured (e.g. genetic) prewiring. Thus, since plasticity is   767
ubiquitous in primate cortex, this suggests that any explanation for the development of   768
head-centred visual responses must utilise a more sophisticated visually-guided learning   769
process than demonstrated by [1], who considered only models with input neurons that   770
were modulated by peaked functions of eye-position. Moreover, the loss of head-centred   771
representations in the manually prewired model by introducing synaptic plasticity also   772
represents a major challenge to the plausibility of previously published models, such as   773
that of [20], which rely on an initial period of supervised learning to establish the   774
required synaptic connectivity. The problem here is that when the supervisory training   775
signal is eventually removed, the continued presence of associative plasticity may   776
degrade and eventually abolish the head-centred output representations.   777

In the remainder of the paper we explore a variety of biologically plausible model   778
variations that are aimed at discovering potential mechanisms by which head-centred   779
output neurons may still develop through visually guided learning even when the   780

network contains input neurons with monotonic modulation by eye-position. We begin ₇₈₁
by exploring the performance of the model when it incorporates a mixture of input ₇₈₂
neurons that are modulated by peaked and sigmoidal eye-position gain fields. After this, ₇₈₃
we explore the operation of the model with a number of more sophisticated, modified ₇₈₄
synaptic learning rules originally developed by [25] in the context of transform invariant ₇₈₅
visual object recognition, which maintain biological plausibility by continuing to rely on ₇₈₆
the locally available activities of the pre- and post-synaptic neurons. The choice of the ₇₈₇
modified versions of the trace learning rule used in the following sections of this paper is ₇₈₈
motivated by the superior performance of these learning rules reported by [25]. Finally, ₇₈₉
we conclude with the investigation of the performance of the model incorporating a ₇₉₀
mixed population of peaked and monotonic modulated visual input neurons with the ₇₉₁
synaptic weights also adjusted using a new modified version trace learning rule. ₇₉₂

Standard Trace Learning Rule with Mixed Peaked and ₇₉₃
Sigmoidal eye-position Modulation of Input Neurons ₇₉₄

In this experiment it is investigated how mixing peaked and sigmoidal gain modulation ₇₉₅
in the input population in varying proportions would influence the development of ₇₉₆
head-centred output neurons in the self-organising model with the standard trace ₇₉₇
learning rule (6). This is an important issue since all cortical areas with eye-position ₇₉₈
gain modulation exhibit a mixture of different forms of modulation [7–9]. A series of ₇₉₉
simulations are conducted where each neuron in the input population is independently ₈₀₀
and randomly set to have either a peaked or sigmoidal gain modulation. Specifically, ₈₀₁
each input neuron is changed from having peaked to sigmoidal modulation with a ₈₀₂
probability p, called the sigmoid modulation rate, and values of $p = 0, 0.1, \ldots, 1.0$ are ₈₀₃
explored. ₈₀₄

The impact of varying the sigmoid modulation rate on the characteristics of the ₈₀₅
model is inspected by plotting key summary statistics as a function of p in Fig 11. As ₈₀₆
expected, the head-centredness rate decreased as the sigmoid modulation rate increased, ₈₀₇
both in the trained and untrained models. However, as long as the sigmoid modulation ₈₀₈
rate is less than 30%, the trained model had a higher proportion of head-centred output ₈₀₉
neurons than the untrained model. In particular, for sigmoid modulation rates less than ₈₁₀
20%, the fraction of head-centred neurons in the trained model did not drop below ₈₁₁
∼15%, and the average head-centredness among head-centred neurons remained no less ₈₁₂
than ∼0.58. ₈₁₃

Fig 11. The effects of incorporating a mixed population of input neurons with both peaked and monotonic eye-position gain modulation. The plots show how the performance metrics vary with the monotonic modulation rate, p, which is the probability of each input neuron having a monotonic eye-position gain modulation. Results are presented showing the response characteristics of the output neurons before training (**A**) and after training (**B**). Conventions are similar to Fig 10. It is evident that the head-centredness rate decreased as the sigmoid modulation rate increased, both in the trained and untrained models. However, as long as the sigmoid modulation rate is less than 30%, the trained model had a higher proportion of head-centred output neurons than the untrained model.

In summary, these results showed that when there is a large proportion of input ₈₁₄
neurons with peaked eye-position gain modulation, say with $0 \leq p \leq 0.2$, then the ₈₁₅
self-organising model is still capable of developing a significant proportion, i.e. no less ₈₁₆
than ∼15%, of head-centred ouput neurons during training. However, as the sigmoid ₈₁₇
modulation rate increased, the performance of the model deteriorated with far fewer ₈₁₈
head-centred output neurons present in the trained model. ₈₁₉

Given that the model incorporating a mixed population of input neurons failed to $\qquad$ 820
develop a significant proportion of head-centred output cells whenever $p > 0.2$, we next $\qquad$ 821
investigated whether the introduction of more powerful, modified synaptic learning rules $\qquad$ 822
could produce head-centred output neurons when the entire population of input neurons $\qquad$ 823
were again modulated by a sigmoidal function of eye-position. Our choice of the $\qquad$ 824
modified versions of the trace learning rule adopted in this paper was motivated by $\qquad$ 825
their superior performance reported in previous work [25]. These modified versions of $\qquad$ 826
the standard trace learning rule are still biologically plausible in terms of only using $\qquad$ 827
locally available signals to update the synaptic weights of connections. Moreover, we $\qquad$ 828
expected that the introduction of a delayed trace of synaptic activity and as well as an $\qquad$ 829
anti-Hebbian component incorporated in these modified versions of the trace learning $\qquad$ 830
rule would provide the model with a way of weakening the observed Hebbian-like $\qquad$ 831
training behaviour evidenced, for example, by the comparison of Fig 7**D** and Fig 7**C**, $\qquad$ 832
and therefore to facilitate the self-organisation of head-centred responses with visual $\qquad$ 833
input neurons with monotonic eye-position gain modulation. The absence of these $\qquad$ 834
components makes other classic Hebbian-based learning rules (e.g. Oja's rule [32]) $\qquad$ 835
ineffective in this case. $\qquad$ 836

Modified Learning Rule: Delayed Postsynaptic Trace with $\qquad$ 837 Anti-Hebbian Learning $\qquad$ 838

[25] investigated how a set of modified more powerful versions of the trace learning rule $\qquad$ 839
can produce improved temporal binding and invariance learning. In particular, the $\qquad$ 840
authors showed that the performance of the trace learning rule is substantially improved $\qquad$ 841
by incorporating a trace of previous neuronal activity with an explicit time delay. This $\qquad$ 842
had the effect of removing the purely Hebbian term of the learning rule [25]. In the next $\qquad$ 843
simulations, the learning rules proposed by [25] were adapted to differential $\qquad$ 844
formulations for the time-continuous scenario in which the simulations are performed. A $\qquad$ 845
Forward Euler scheme was used to numerically integrate the differential equations. In $\qquad$ 846
all simulations the numerical time step was kept as one tenth of the neuronal time $\qquad$ 847
constant τ_h. Unless explicitly mentioned, the learning rule was the only change from $\qquad$ 848
previous simulations. $\qquad$ 849

This section presents simulation results showing the performance of a modified $\qquad$ 850
learning rule incorporating a delayed postsynaptic trace with anti-Hebbian learning [33]. $\qquad$ 851
We investigate the impact of this learning rule on the self-organisation of the synaptic $\qquad$ 852
weights and firing rate responses of the output neurons when all input neurons were $\qquad$ 853
modulated by sigmoidal eye-position gain fields. The learning rule was defined by $\qquad$ 854

$$\frac{dw_{ij}(t)}{dt} = \alpha \left(\beta q_i(t - \Delta T) - y_i(t) \right) v_j(t) \qquad (16)$$

where y_i and v_j were, respectively, the post and presynaptic firing rate values, α was the $\qquad$ 855
learning rate, β was an unconstrained tuning parameter, and q_i was the trace value of $\qquad$ 856
the output neuron i calculated according to Eq 5 at time $(t - \Delta T)ms$. Eq 16 resembles $\qquad$ 857
a form of error-correction learning where the delayed-trace term $\beta q_i(t - \Delta T)$ is the $\qquad$ 858
target for the current postsynaptic firing rate. The learning rule is biologically plausible $\qquad$ 859
in that it utilises only the local activities of the pre- and post-synaptic neurons. $\qquad$ 860
Expanding Eq 16 will result in $\qquad$ 861

$$\frac{dw_{ij}(t)}{dt} = \alpha \left(\beta q_i(t - \Delta T) - y_i(t) \right) v_j(t) \qquad (17)$$

where $\alpha \beta q_i(t - \Delta T) v_j(t)$ is the *delayed-trace term* of the learning rule. This is the term $\qquad$ 862
which contains the tuning parameter β. The remaining term $-\alpha y_i(t) v_j(t)$ is minus the $\qquad$ 863

learning rate α times the product of the post and presynaptic firing rates y_i and v_j,   864
respectively. This term is referred to as the *anti-Hebbian term* of the learning rule.   865

    The behaviour of the learning rule shown in Eq 16 is governed by scaling the   866
parameter β. Scaling β up could result in the delayed-trace component dominating the   867
learning rule and, therefore, resulting in the same trace-like training behaviour   868
described in previous sections. Similarly, scaling β down could make the anti-Hebbian   869
term dominate the behaviour of the learning rule and consequently lead to a qualitative   870
change in the final outcome of the training.   871

    The parameters for the model are given in Table 1. The model was trained   872
according to the description given in section The Visually-Guided Training of the   873
Network. Likewise, in all cases the model was tested on the same visual stimuli. The   874
time delay ΔT used to compute the trace value of each output neuron and the   875
parameter β were both tuned to optimise the performance of the model at developing   876
head-centred output neurons. The time delay ΔT used to compute the trace value of   877
each output neuron i was $50ms$. The parameter β was set to 2.2.   878

    Fig 12 shows the firing rate responses of output neuron #168 before and after   879
training, with results shown for four different eye-positions. The miniature scatter plots   880
presented within each of the two subplots **A** and **B** show the reference frame values of   881
all neurons in the output layer. Neuron #168 is indicated in the scatter plots by a red   882
mark. Fig 12**A** shows that prior to training the response of output neuron #168 had no   883
consistent structure in head-centred space across different eye-positions. However,   884
Fig 12**B** shows that after training the output neuron responded maximally to the same   885
head-centred location across all four eye-positions. This neuron has thus learned to   886
respond in a head-centred reference frame.   887

Fig 12. Simulation results showing the firing rate responses of a model incorporating a population of monotonic modulated input neurons trained with the modified learning rule 16: Delayed Postsynaptic Trace with anti-Hebbian Learning. The figure shows the firing rate responses of output neuron #168 before training (**A**) and after training (**B**) during testing for four different eye-positions: $-18°, -6°, 6°$ and $18°$. In each subplot, each curve corresponds to a fixed eye-position while a visual target is presented across the same range of head-centred locations. The miniature scatter plot shows the reference frame values of all neurons in the output layer, where each neuron is plotted as a point corresponding to that neuron's particular combination of head-centredness (ordinate) and eye-centredness (abscissa). The neuron whose firing rate responses have been plotted is shown in the scatter plot by a red mark. After training it is evident that this neuron responds reasonably invariantly to a visual target presented at the same head-centred location regardless of the eye-position.

    The change in the synaptic weight structure of the same output neuron #168 due to   888
training is shown in Fig 13. Before training started the afferent synaptic weights were   889
randomly assigned (Fig 13**A**). Fig 13**B** shows that after training, in contrast to the   890
horizontal structure previously obtained with the standard trace learning rule shown in   891
Fig 7**D**, the structure obtained with the modified learning rule 16 is similar to the   892
predicted structure shown in Fig 8 for a head-centred neuron.   893

    Fig 14 presents a population analysis of the reference frame response characteristics   894
of the output neurons before and after training. In particular, the scatter plot in Fig 14   895
shows that before training nearly all of the output neurons had head-centredness values   896
close to 0 and were classified as eye-centred. However, after training the   897
head-centredness values of many output neurons had dramatically increased, with quite   898
a number of these neurons now classed as head-centred. Comparing the output   899
population analysis of the model trained with the modified learning rule 16 shown in   900

Fig 13. Simulation results showing the strengths of the afferent synapses of a model incorporating a population of sigmoidal modulated input neurons trained with the modified learning rule 16: Delayed Postsynaptic Trace with anti-Hebbian Learning. The figure shows the strengths of the afferent synapses from the input population to output neuron #168 for the untrained **(A)** and trained **(B)** model. The output neuron corresponds to the one plotted in Fig 12. In each plot, the afferent synapses have been arranged topographically by the preference of the input neuron for retinal location α_i and eye-position β_j. The portion of each plot to the left of the white dashed line corresponds to input neurons with positive gain $\kappa_j > 0$, whilst the portion of each plot to the right of the white dashed line corresponds to those input neurons with negative gain $\kappa_j < 0$. The synaptic weights for this output neuron after training **(B)** have approximately the correct structure for a head-centred neuron as shown in Fig 8.

Fig 14 with the performance of the model trained with the standard trace learning rule (6) shown in Fig 5 confirms that the new modified learning rule 16 is far more efficacious at driving the development of head-centred output neurons when the input neurons are modulated by a sigmoidal (monotonic) function of eye-position than the standard trace learning rule (6) originally investigated by [1].

Fig 14. Simulation results showing the output reference frame response characteristics of a model incorporating a population of sigmoidal modulated input neurons trained with the modified learning rule 16: Delayed Postsynaptic Trace with anti-Hebbian Learning. The scatter plot shows the reference frame response characteristics of all output neurons before and after training. Each neuron is represented as a point corresponding to its combination of eye-centredness (abscissa) and head-centredness (ordinate) values. Data points for the untrained model are plotted in blue and data points for the trained model are shown in red. The dashed diagonal line with positive unity slope separates those neurons which are classified as head-centred (above the line) from those that are classified as eye-centred (below the line). It can be seen that many of the output neurons have developed head-centred output responses after training.

In summary, these results showed that training the model with the modified learning rule 16 refined the response characteristics of many output neurons to be more compatible with a head-centred frame of reference, even when all of the input neurons had monotonic eye-position gain modulation.

Modified Learning Rule: Delayed Postsynaptic Firing Rate with Anti-Hebbian Learning

This section presents simulation results showing the performance of a learning rule which incorporates a delayed postsynaptic firing rate with anti-Hebbian learning [25]. The same training procedure of previous simulations was used in the simulations presented in this section. The learning rule is defined by

$$\frac{dw_{ij}(t)}{dt} = \alpha \left(\beta y_i(t - \Delta T) - y_i(t) \right) v_j(t) \tag{18}$$

where y_i was the firing rate of output neuron i. In this case no postsynaptic trace value q_i is used to update the synaptic weights. The tuning parameter β works as described in section Modified Learning Rule: Delayed Postsynaptic Trace with Anti-Hebbian Learning for the anti-Hebbian learning rule with delayed trace (Eq 16). The time delay

ΔT in the firing rate of each output neuron and the parameter β were both tuned to 920
optimise the performance of the model in driving the development of head-centred 921
output neurons. The value of the time delay ΔT was set to $500ms$ and β was set to 2.4. 922
Simulation parameters for the model are shown in Table 1. 923

Fig 15 shows the firing rate responses of output neuron #876 before training 924
(Fig 15**A**) and after training (Fig 15**B**). Fig 15**B** shows that after training output 925
neuron #876 responded to the same head-centred location across different eye-positions. 926
This was not the case for the same output neuron before training (Fig 15**A**). Thus, it is 927
evident that during training the neuron has learned to respond in a head-centred 928
reference frame. 929

**Fig 15. Simulation results showing the firing rate responses of a model
incorporating a population of monotonic modulated input neurons trained
with the modified learning rule 18: Delayed Postsynaptic Firing Rate with
anti-Hebbian Learning.** The figure shows the firing rate responses of output neuron
#876 before training **(A)** and after training **(B)** during testing for four different
eye-positions: $-18°, -6°, 6°$ and $18°$. Conventions as for Fig 12. The comparison of
subplot **(A)** and subplot **(B)** shows that the output neuron learned to respond to a
specific head-centred location regardless of the eye-position after training.

Fig 16 shows how the synaptic weight structure of the same output neuron #876 930
changed due to training the model with learning rule 18. The final weight structure 931
after training shown in Fig 16**B** resembles the predicted weight structure shown in Fig 8 932
for head-centred neurons. 933

**Fig 16. Simulation results showing the strengths of the afferent synapses of
a model incorporating a population of sigmoidal modulated input neurons
trained with the modified learning rule 18: Delayed Postsynaptic Firing
Rate with anti-Hebbian Learning.** The figure shows the strengths of the afferent
synapses from the input population to output neuron #876 for the untrained **(A)** and
trained **(B)** model. The output neuron corresponds to the one plotted in Fig 15.
Conventions as for Fig 13. The synaptic weight structure for this output neuron after
training shown in plot **(B)** has approximately the correct profile for a head-centred
neuron (Fig 8).

Fig 17 shows the eye-centredness and head-centredness values of output neurons in 934
the untrained and in the trained model. It is clear that almost none of the output 935
neurons in the untrained model had values of head-centredness higher than 936
eye-centredness. However, after training the head-centredness values of many output 937
neurons increased substantially, with a number of such neurons now having greater 938
head-centredness than eye-centredness values. Such neurons are, therefore, classified as 939
head-centred neurons (section Analysis of Network Performance). Comparing the 940
output population analysis of the model trained with the modified learning rule 18 941
shown in Fig 17 with the analysis of the model trained with the standard trace learning 942
rule (6) shown in Fig 5 demonstrates that the new modified learning rule 18 is also 943
more efficacious at producing head-centred output neurons when the input neurons are 944
modulated by a sigmoidal function of eye-position than the standard trace learning 945
rule (6) previously implemented by [1]. 946
In summary, these results showed that training the model with the modified learning 947
rule 18 resulted in the development of head-centred output neurons, even when the 948
whole input population had sigmoidal eye-position gain modulation. However, the 949
comparison of Fig 17 and Fig 14 shows that learning rule 16, which incorporated a 950
delayed postsynaptic trace $q_i(t - \Delta T)$, is in fact more efficacious at driving the 951

Fig 17. Simulation results showing the output reference frame response characteristics of a model incorporating a population of sigmoidal modulated input neurons trained with the modified learning rule 18: Delayed Postsynaptic Firing Rate with anti-Hebbian Learning. The scatter plot shows the reference frame response characteristics of all output neurons before and after training. Conventions as for Fig 14. It is evident that training had the effect of increasing the head-centredness values of most output neurons. Indeed many more head-centred output neurons are present in the trained model than in the untrained model.

development of head-centred output neurons than learning rule 18, which incorporated   952
the delayed firing rate $y_i(t - \Delta T)$. Thus, the incorporation of the trace value $q_i(t - \Delta T)$ 953
enhances the ability of the learning rule to perform temporal binding of input patterns   954
corresponding to the same head-centred location.   955

Modified Learning Rule: Current Postsynaptic Trace with   956
Anti-Hebbian Learning   957

This section presents simulation results showing the performance of a modified learning   958
rule which incorporated the current postsynaptic trace with anti-Hebbian learning.   959
Thus, this learning rule does not use an explicit time delay ΔT. The learning rule was   960
given by   961

$$\frac{dw_{ij}(t)}{dt} = \alpha \left(\beta q_i(t) - y_i(t) \right) v_j(t) \tag{19}$$

where α was the learning rate, β was the tuning parameter, q_i was the trace value of the   962
output neuron i, and y_i and v_j were the post- and pre-synaptic firing rate values,   963
respectively. What distinguishes the learning rule in Eq 19 from the learning rule in   964
Eq 16 is the use of the trace value calculated at the same time t when the synaptic   965
weight is updated.   966

Table 1 gives the parameters for the model. The value of the tuning parameter β 967
was set to 2.2 for optimal performance.   968

Fig 18 shows the firing rate responses of output neuron #328 for the untrained and   969
trained models. Specifically, Fig 18**A** shows that prior to training the response of   970
output neuron #328 had no consistent structure in head-centred space across different   971
eye-positions. However, Fig 18**B** shows that after training the same output neuron   972
reponded maximally to the same head-centred location across all four eye-positions.   973
Thus, after training, neuron #328 responded in a head-centred frame of reference.   974

Fig 18. Simulation results showing the firing rate responses of a model incorporating a population of monotonic modulated input neurons trained with the modified learning rule 19: Current Postsynaptic Trace with anti-Hebbian Learning. The figure shows the firing rate responses of output neuron #328 before training (**A**) and after training (**B**) during testing for four different eye-positions: $-18°, -6°, 6°$ and $18°$. Conventions as for Fig 12. The comparison of subplot (**A**) and subplot (**B**) shows that the output neuron learned to respond to a specific head-centred location regardless of the eye-position after training.

The change in the synaptic weight structure of the same output neuron #328 due to   975
training is shown in Fig 19. Before training the afferent synaptic weights were randomly   976
assigned (Fig 19**A**). After training, however, the synaptic weight structure of the same   977

output neuron (Fig 19**B**) is similar to the predicted weight structure for head-centred   978
neurons shown in Fig 8.   979

Fig 19. Simulation results showing the strengths of the afferent synapses of a model incorporating a population of sigmoidal modulated input neurons trained with the modified learning rule 19: Current Postsynaptic Trace with anti-Hebbian Learning. The figure shows the strengths of the afferent synapses from the input population to output neuron #328 for the untrained (**A**) and trained (**B**) model. The output neuron corresponds to the one plotted in Fig 18. Conventions as for Fig 13. The synaptic weight structure for this output neuron after training shown in plot (**B**) has the correct kind of profile for a head-centred neuron (Fig 8).

Fig 20 shows the eye-centredness and head-centredness values of output neurons in   980
the untrained and in the trained model. In particular, Fig 20 shows that training had   981
the effect of increasing the head-centredness value for a large proportion of output   982
neurons. Furrthermore, while almost no output neurons were classified as head-centred   983
before training, a significant number of output neurons were classified as head-centred   984
after training. A comparison of the output population analysis of the model trained   985
with the modified learning rule 19 shown in Fig 20 with the performance of the model   986
trained with the standard trace learning rule (6) presented in Fig 5 shows that the   987
modified learning rule 19 is also significantly more capable of producing head-centred   988
output neurons than the standard trace learning rule (6) when all of the input neurons   989
have sigmoidal gain modulation by eye-position.   990
In summary, these results showed that training the model with learning rule 19   991
drives the development of head-centred output neurons even when the whole input   992
population had sigmoidal eye-position gain modulation. The comparison of Fig 20 with   993
Fig 14 shows that learning rule 16, which incorporated a delayed postsynaptic trace   994
$q_i(t - \Delta T)$, is more effective at producing head-centred output neurons than learning   995
rule 19, which incorporated the current trace $q_i(t)$ calculated at the same time t when   996
the weights are updated.   997

Fig 20. Simulation results showing the output reference frame response characteristics of a model incorporating a population of sigmoidal modulated input neurons trained with the modified learning rule 19: Current Postsynaptic Trace with anti-Hebbian Learning. The scatter plot shows the reference frame response characteristics of all output neurons before and after training. Conventions as for Fig 14. It can be seen that training increased the head-centredness values of most output neurons, with quite a number of head-centred output neurons present in the trained model.

Modified Learning Rule: Delayed Postsynaptic Trace Learning   998
Rule   999

The simulation results presented in section Modified Learning Rule: Delayed   1000
Postsynaptic Trace with Anti-Hebbian Learning, section Modified Learning Rule: 1001
Delayed Postsynaptic Firing Rate with Anti-Hebbian Learning and section Modified   1002
Learning Rule: Current Postsynaptic Trace with Anti-Hebbian Learning showed,   1003
respectively, that training the model with learning rule 16, learning rule 18 and learning   1004
rule 19 successfully self-organised head-centred output responses and increased the   1005
head-centredness value of a large proportion of output neurons when all input neurons   1006
had sigmoidal eye-position gain modulation. Importantly, section Self-organisation with   1007
peaked and monotonic gain fields showed this was not the case for the standard trace   1008

learning rule (6). Training the model with the standard trace learning rule successfully self-organised head-centred output neurons when all of the input neurons had peaked eye-position gain modulation, but failed when the modulation of the input population was altered from peaked to sigmoidal. Indeed, the simple introduction of a small proportion (e.g. with $p > 0.2$) of input neurons with sigmoidal eye-position gain modulation was enough to undermine the self-organisation of head-centred output responses (section Standard Trace Learning Rule with Mixed Peaked and Sigmoidal eye-position Modulation of Input Neurons).

The modified learning rules introduced in section Modified Learning Rule: Delayed Postsynaptic Trace with Anti-Hebbian Learning, section Modified Learning Rule: Delayed Postsynaptic Firing Rate with Anti-Hebbian Learning and in section Modified Learning Rule: Current Postsynaptic Trace with Anti-Hebbian Learning all had an anti-hebbian term as their common component. Out of these learning rules, the best performance was observed with learning rule 16, which incorporated a postsynaptic delayed-trace term. In this case, an interesting question is whether the superior efficacy of this learning rule in driving the development of head-centred output responses was primarily due to the anti-hebbian term or the postsynaptic delayed-trace term. In particular, is an anti-hebbian term actually needed in this learning rule for the self-organisation of head-centred responses in the presence of input neurons with sigmoidal eye-position gain modulation, or could head-centred output responses develop using a learning rule that only incorporated a postsynaptic delayed-trace term?

This section addresses the above questions by investigating the performance of the model with the following learning rule

$$\frac{dw_{ij}(t)}{dt} = \alpha q_i(t - \Delta T)v_j(t) \qquad (20)$$

where α was the learning rate, q_i was the trace value of the output neuron i and v_j was the firing rate of the input neuron j. In Eq 20 the trace value q_i is calculated at time $(t - \Delta T)ms$. This learning rule has no anti-hebbian term, and relies purely on the postsynaptic delayed-trace term $q_i(t - \Delta T)$ to drive the development of head-centred output neurons.

The simulation parameters for the model are given in Table 1. The time delay ΔT used to compute the trace value of each output neuron i was set to $30ms$ for optimal learning performance.

Fig 21 shows how training changed the firing rate responses of output neuron #223. Prior to training the response of output neuron #223 had no consistent structure in head-centred space across different eye-positions (Fig 21**A**), whilst after training the same output neuron responded maximally to the same head-centred location across all four eye-positions (Fig 21**B**). Thus, neuron #223 learned to respond in a head-centred reference frame after training.

Fig 22 shows how the synaptic weight structure of the same output neuron #223 plotted in Fig 21 changed due to training the model with learning rule 20. It is clear that the final synaptic weight structure after training (Fig 22**B**) resembles the predicted weight structure for head-centred neurons (Fig 8), even though this was not the case before training (Fig 22**A**).

Fig 23 shows the eye-centredness and head-centredness values of all of the output neurons in the untrained model and in the trained model. After training, the head-centredness values of many output neurons had increased substantially. However, there was only a single output neuron, which was neuron #223, with a greater head-centredness value than eye-centreredness, and which was consequently classed as responding in a head-centred reference frame. Therefore, in the simulations presented in this paper, the anti-hebbian term in learning rules (16), (18) and (19) appears to play

Fig 21. Simulation results showing the firing rate responses of a model incorporating a population of monotonic modulated input neurons trained with the modified learning rule 20: Delayed Postsynaptic Trace Learning Rule. The figure shows the firing rate responses of output neuron #223 before training (**A**) and after training (**B**) during testing for four different eye-positions: $-18°, -6°, 6°$ and $18°$. Conventions as for Fig 12. The comparison of subplot (**A**) and subplot (**B**) shows that the output neuron learned to respond to a specific head-centred location regardless of the eye-position after training. Output neuron #223 is not shown in the scatter plot of subplot (**A**) because this neuron did not respond for every eye-position before training and was therefore excluded from further analysis (section Analysis of Network Performance). However, subplot (**B**) shows that the same output neuron learned to respond to a specific head-centred location regardless of the eye-position after training.

Fig 22. Simulation results showing the strengths of the afferent synapses of a model incorporating a population of sigmoidal modulated input neurons trained with the modified learning rule 20: Delayed Postsynaptic Trace Learning Rule. The figure shows the strengths of the afferent synapses from the input population to output neuron #223 for the untrained (**A**) and trained (**B**) model. The output neuron corresponds to the one plotted in Fig 21. Conventions as for Fig 13. The synaptic weight structure for this output neuron after training shown in plot (**B**) has approximately the correct profile for a head-centred neuron (Fig 8).

an important and essential role in producing relatively large numbers of head-centred ₁₀₅₈ output neurons when all of the input neurons have sigmoidal eye-position gain fields. ₁₀₅₉

Fig 23. Simulation results showing the output reference frame response characteristics of a model incorporating a population of sigmoidal modulated input neurons trained with the modified learning rule 20: Delayed Postsynaptic Trace Learning Rule. The scatter plot shows the reference frame response characteristics of all output neurons before and after training. Conventions as for Fig 14. It is evident that training had the effect of increasing the head-centredness values of most output neurons. Although, there is only a single head-centred output neuron present in the trained model.

Delayed Postsynaptic Trace Learning Rule with Mixed Peaked ₁₀₆₀ and Sigmoidal eye-position Modulation of Input Neurons ₁₀₆₁

In the previous section, it was found that an anti-hebbian term was needed in the ₁₀₆₂ learning rule in order to produce relatively large numbers of head-centred output ₁₀₆₃ neurons if the entire population of input neurons had sigmoidal gain fields. However, ₁₀₆₄ experimental studies have demonstrated that the primate cortex contains a mixed ₁₀₆₅ population of visual neurons with either peaked or monotonic eye-position gain ₁₀₆₆ fields [7–9]. This raises the question of whether learning rule (20), which relies solely on ₁₀₆₇ a postsynaptic delayed-trace term without any anti-hebbian term, could produce a ₁₀₆₈ much larger number of head-centred output neurons if the input population had a 50:50 ₁₀₆₉ mix of peaked and sigmoidal eye-position gain fields. ₁₀₇₀

This section presents simulation results with the modified learning rule (20) when ₁₀₇₁ there is a 50:50 mixture of peaked and monotonic gain fields in the visual input ₁₀₇₂ population. Can the model produce a large number of head-centred output neurons ₁₀₇₃ under such conditions without an anti-hebbian term in the learning rule? This is still a ₁₀₇₄

potentially challenging task for the model because in section Standard Trace Learning ₁₀₇₅ Rule with Mixed Peaked and Sigmoidal eye-position Modulation of Input Neurons it ₁₀₇₆ was shown that the standard trace learning rule (6), which lacks an anti-hebbian term, ₁₀₇₇ failed to produce significant numbers of head-centred output neurons when the ₁₀₇₈ proportion of sigmoidal gain modulated input neurons rose above just 20% of the overall ₁₀₇₉ input population. The model parameters for the simulations presented in this section ₁₀₈₀ are given in Table 1. ₁₀₈₁

Fig 24 shows how training changed the firing rate responses of output neuron #281. ₁₀₈₂ In particular, Fig 24**B** shows that after training output neuron #281 responded ₁₀₈₃ maximally to the same head-centred location across all four eye-positions, although this ₁₀₈₄ was not the case prior to training (Fig 24**A**). Hence neuron #281 responded in a ₁₀₈₅ head-centred frame of reference after training. ₁₀₈₆

Fig 24. Simulation results of a model incorporating a mixed population of peaked and sigmoidal modulated input neurons, with sigmoidal modulation rate p set to 0.5, trained with the modified learning rule 20: Delayed Postsynaptic Trace Learning Rule. The figure shows the firing rate responses of output neuron #281 before training **(A)** and after training **(B)** during testing for four different eye-positions: $-18°, -6°, 6°$ and $18°$. Conventions as for Fig 12. Plot **(B)** shows that the same output neuron learned to respond to a specific head-centred location regardless of the eye-position after training.

Fig 25 shows how the synaptic weight structure of the same output neuron #281 ₁₀₈₇ plotted in Fig 24 changed due to training. Fig 25**B** shows that after training, the ₁₀₈₈ synaptic weight structure of the output neuron was clearly similar to the predicted ₁₀₈₉ weight structure for head-centred neurons shown in Fig 8. The synaptic weight ₁₀₉₀ structure before training reflected the randomly assigned connection weights (Fig 25**A**). ₁₀₉₁

Fig 25. Simulation results of a model incorporating a mixed population of peaked and sigmoidal modulated input neurons, with sigmoidal modulation rate p set to 0.5, trained with the modified learning rule 20: Delayed Postsynaptic Trace Learning Rule. The figure shows the strengths of the afferent synapses from the input population to output neuron #281 for the untrained **(A)** and trained **(B)** model. The output neuron corresponds to the one plotted in Fig 24. Conventions as for Fig 13. The synaptic weight structure for this output neuron after training shown in plot **(B)** has the correct kind of profile for a head-centred neuron (Fig 8).

Fig 26 shows the eye-centredness and head-centredness values of output neurons in ₁₀₉₂ the untrained and in the trained model. Fig 26 shows that training the model with ₁₀₉₃ learning rule 20, where the input population contained a 50:50 mix of neurons with ₁₀₉₄ peaked or sigmoidal gain modulation, had the effect of increasing the head-centredness ₁₀₉₅ value of most output neurons. Moreover, a large proportion of output neurons in the ₁₀₉₆ trained model are head-centred (i.e. with a head-centredness value greater than ₁₀₉₇ eye-centredness). Indeed, more head-centred output neurons were observed in the ₁₀₉₈ trained model in this section than in any of the trained models presented in previous ₁₀₉₉ section Modified Learning Rule: Delayed Postsynaptic Trace with Anti-Hebbian ₁₁₀₀ Learning, section Modified Learning Rule: Delayed Postsynaptic Firing Rate with ₁₁₀₁ Anti-Hebbian Learning and section Modified Learning Rule: Current Postsynaptic ₁₁₀₂ Trace with Anti-Hebbian Learning. ₁₁₀₃

In summary, these results demonstrated that it was possible for the model to ₁₁₀₄ produce large numbers of head-centred output neurons with a learning rule that relied ₁₁₀₅ purely on a postsynaptic delayed-trace term without any anti-hebbian term if the input ₁₁₀₆

Fig 26. Simulation results of a model incorporating a mixed population of peaked and sigmoidal modulated input neurons, with sigmoidal modulation rate p set to 0.5, trained with the modified learning rule 20: Delayed Postsynaptic Trace Learning Rule. The scatter plot shows the reference frame response characteristics of all output neurons before and after training. Conventions as for Fig 14. It is evident that training had the effect of increasing the head-centredness values of most output neurons, with many more head-centred output neurons present in the trained model.

population contained a 50:50 mix of neurons that were modulated by either peaked or   1107
sigmoidal gain fields. Such a mixture of different forms of eye-position gain modulation   1108
is biologically compatible with experimental findings [7,8].   1109

Discussion   1110

The majority of previously published models of coordinate transformation from   1111
eye-centred to head-centred visual representations have relied on some form of   1112
supervised error-correction learning, in which an explicit supervisory signal is used to   1113
specify the desired head-centred output responses during training [14–16]. The   1114
availability of such a supervisory training signal makes the self-organisation of these   1115
models robust even with monotonic (e.g. planar or sigmoidal) eye-position gain   1116
modulated input neurons. However, an immediate problem with these kinds of models   1117
is explaining exactly where such a supervisory training signal might originate from in   1118
the brain. Another major problem for models that employ a backpropagation of error   1119
supervised learning, such as the classic model of [14], is that this model architecture is   1120
entirely biologically implausible [18]. In particular, there is no plausible explanation for   1121
how the error terms needed to adjust the afferent synaptic weights in the intermediate   1122
layer of the model could be generated and implemented in the brain. One consequence   1123
of this is that the backpropagation of error learning procedure can result in individual   1124
neurons making both excitatory and inhibitory synaptic connections on different   1125
postsynaptic neurons. Although not shown here, we have verified this through   1126
replicating the model simulations of [14] and [16]. This feature of backpropagation of   1127
error models violates an accepted principle of cortical architecture, sometimes referred   1128
to as Dale's Law, that an individual neuron must have the same kind of excitatory or   1129
inhibitory effect at all of its synaptic connections with other neurons [19]. This failure   1130
of backpropagation of error models even undermines the potential relevance of their   1131
trained synaptic architecture to understanding how coordinate transformations to   1132
head-centred visual representations might be implemented in the brain. [15] also used   1133
error-correction learning to develop head-centred output representations. Their learning   1134
scheme employed a simpler global error signal for the entire output population, which   1135
might conceivably be implemented by some form of neuromodulator release. However,   1136
the implementation of error correction learning in their model still required complex   1137
architectural features that have not been identified in cortex.   1138
　　To remedy the lack of biological plausibility in previously published models that use   1139
supervised learning to drive the development of visual neurons that respond in a   1140
head-centred reference frame, [1] demonstrated a model that self-organised using   1141
unsupervised competitive learning driven by the standard trace learning rule (6). In   1142
their model the trace learning rule was able to exploit the natural statistics of how   1143
primates tend to move their eyes and head as they explore their visual environment,   1144
with more frequent shifts in eye-position than head position. These natural eye and   1145
head movements enable trace learning to bind together different visual input patterns   1146

corresponding to visual targets located in the same head-centred location but different 1147 retinal locations, thereby driving the development of postsynaptic neurons that respond 1148 to visual targets in specific head-centred locations. 1149

It was originally demonstrated by [1], and shown again above, that the 1150 self-organising model described in section Materials and methods using the standard 1151 trace learning rule (6) with peaked eye-position gain modulated input neurons is able to 1152 develop head-centred output representations during training. However, a key new result 1153 in this paper is that the self-organising model with purely sigmoidal eye-position gain 1154 modulated input neurons develops eye-centred output neurons when using the standard 1155 trace learning rule. The cause of this contrasting behaviour between peaked and 1156 sigmoidal gain fields is the correlations between the activity of the input neurons across 1157 all of the input patterns during training. It is well understood that in a standard 1158 competitive neural network, individual output neurons learn to respond to subsets of 1159 input neurons that tend to be most frequently co-active [18]. In the self-organising 1160 model with peaked gain modulation, the subsets of input neurons that are frequently 1161 co-active correspond to circular clusters that are highly localised in both the retinotopic 1162 preference and eye-position preference dimensions. With a standard hebbian learning 1163 rule with no significant memory trace of recent neuronal activity, individual output 1164 neurons will learn to respond to these localised circular clusters of input neurons. If a 1165 trace learning rule is implemented, it is a relatively easy task for individual output 1166 neurons to simply bind together these clusters of input neurons along a diagonal line in 1167 the input space corresponding to a particular head-centred location. Output neurons 1168 will then respond to particular head-centred locations regardless of eye-position or the 1169 retinal location of a visual target. However, the situation is quite different with 1170 sigmoidal gain modulated input neurons. Due to monotonic saturation of the input 1171 neuron response function in the eye-position dimension of the input space, the subsets 1172 of input neurons that are most frequently co-active are localised in the retinotopic 1173 preference dimension but elongated in the eye-position preference dimension. With a 1174 standard hebbian learning rule, individual output neurons will learn to respond to these 1175 elongated clusters of input neurons, which will give rise to eye-centred output responses. 1176 However, if a trace learning rule is implemented, the output neurons still learn to 1177 represent eye-centred rather than head-centred locations. This is because developing 1178 head-centred output responses would require the trace learning rule to disrupt and 1179 break apart output representations corresponding to the elongated clusters of input 1180 neurons with correlated activities. However, in practice the trace learning effect is not 1181 strong enough to achieve this. Consequently, even with trace learning, the elongated 1182 clusters of input neurons with correlated activities continue to drive the development of 1183 eye-centred output neurons. This finding holds for any input neuron response function 1184 with a monotonic gain in the eye-position dimension, be it purely linear [14] or linear 1185 rectified [20]. 1186

We next showed that a manually prewired neural network model with sigmoidal 1187 eye-position gain modulated input neurons could perform the coordinate transformation. 1188 This is achieved by elevating the weight of synaptic connections from all input neurons 1189 which responded strongly, for some eye-position, to a visual target in the head-centred 1190 location to which the postsynaptic output neuron is assigned. This result established 1191 the feasability of the coordinate transformation within the given model architecture 1192 with sigmoidal gain fields acting on the input population. However, when synaptic 1193 plasticity based on the standard trace learning rule (6) is suddenly introduced into the 1194 manually prewired model, it is found that just a single epoch of visually-guided training 1195 is sufficient to dramatically reduce the prevalence of head-centred neurons in the output 1196 population, and by the 5th epoch all neurons are eye-centred for all subsequent epochs 1197 of training. This showed that sigmoidal gain modulation would, in so far as the 1198

synapses are plastic, even undermine the functioning of a cortical circuit which is 1199
somehow prewired, perhaps by genetic hardwiring or by an initial period of supervised 1200
learning as suggested by [20], to produce the head-centred visual representations. Given 1201
the ubiquitous presence of associative synaptic plasticity in cortex, it is therefore a 1202
substantial challenge to explain how head-centred visual neurons might develop and 1203
persist in the brain given the relatively large proportion of precursor eye-centred visual 1204
neurons that have monotonic eye-position gain fields. 1205

It has been shown that neurons in many parietal areas have a mixture of different 1206
forms of gain modulation, not all of which are planar. In fact, 41% and 56% are not 1207
planar in areas LIP and 7a, respectively [8]. Consequently, we explored how various 1208
degrees of prevalence of sigmoidal gain modulation would influence the self-organisation 1209
of the model with the standard trace learning rule (6). It is found that so long as there 1210
is no more than approximately 20% sigmoidal gain modulation in the input population 1211
then the fraction of head-centred neurons in the trained model did not drop below 1212
$\sim$15%. However, the decrease in performance, and eventual collapse of the model, is 1213
very severe when the presence of sigmoidal gain modulation in the input population is 1214
increased. In particular, with a more biologically realistic 50:50 mix in peaked and 1215
sigmoidal gain modulated input neurons, the model failed to develop a significant 1216
population of head-centred output neurons with the standard trace learning rule (6). 1217

In order to find a biologically plausible way in which the self-organising model could 1218
develop relatively large numbers of head-centred visual output neurons when at least 1219
half or even all of the input neurons had sigmoidal gain fields, we next explored the 1220
performance of the model architecture using a variety of more sophisticated learning 1221
rules that may incorporate temporally delayed memory traces, as well as a mixture of 1222
both trace learning and anti-Hebbian learning terms. These new, modified learning 1223
rules were previously developed by [25] in the context of modelling transform invariant 1224
visual object recognition. The new learning rules continue to be biologically plausible 1225
because they rely on locally available biological quantities, namely the activities of the 1226
pre- and post-synaptic neurons, to guide the modification of synaptic weights. The 1227
different modified learning rules were found to successfully drive the self-organisation of 1228
head-centred output responses when all of the input neurons had sigmoidal eye-position 1229
modulation. The modified learning rules were able to substantially improve the 1230
temporal binding of the standard trace learning rule by incorporating a trace of 1231
previous neuronal activity with an explicit time delay ΔT. This was evidenced by 1232
better performance being achieved when the learning rule incorporated a trace value of 1233
the postsynaptic neuron from an earlier time ΔT in the past instead of the trace value 1234
at the current time. Furthermore, the new learning rules were able to overcome the high 1235
correlations between overlapping input patterns with sigmoidal gain fields through the 1236
additional incorporation of anti-Hebbian learning, which had been previously found to 1237
offer a significant performance enhancement by [25]. However, learning rule (20) 1238
incorporated a delayed postsynaptic trace without an anti-Hebbian term 1239
(section Modified Learning Rule: Delayed Postsynaptic Trace Learning Rule). 1240
Simulation results with this learning rule showed that head-centred output responses 1241
developed in the trained model. Thus, anti-Hebbian learning is not necessarily a 1242
requirement for the development of head-centred output responses. The performance of 1243
learning rule (20) was then investigated under a more biologically realistic scenario in 1244
which the input population consisted of a 50:50 mixture of neurons with either peaked 1245
or sigmoidal eye-position gain modulation. These results demonstrated that the model 1246
could produce large numbers of head-centred output neurons with a learning rule that 1247
relied purely on a postsynaptic delayed-trace term without any anti-hebbian term if the 1248
input population contained a 50:50 mix of neurons modulated by either peaked or 1249
sigmoidal gain fields. These last findings should be contrasted with the performance of 1250

the model with the standard trace learning rule (6), which failed to develop a significant number of head-centred output neurons with such a mixed input population.

Conclusion

In conclusion, the work presented here has shown that the existence of a synaptic weight structure that can perform a coordinate transformation does not guarantee that it will emerge through a process of self-organisation using any one particular form of trace learning rule. In particular, the standard trace learning rule originally proposed by [1] failed to produce head-centred output neurons when the input neurons were modulated by a sigmoidal function of eye-position, and even failed with a biologically realistic 50:50 mix of input neurons with peaked and sigmoidal gain fields. In order to remedy this problem, we had to investigate the use of more sophisticated, yet still biologically plausible, learning rules that incorporated temporally delayed memory traces, as well as a mixture of both trace learning and anti-hebbian learning terms. These new, modified learning rules were found to produce head-centred output neurons when the input population had sigmoidal gain fields. Moreover, it was also found that the delayed postsynaptic trace in learning rule (20) was sufficient to drive the development of head-centred output neurons in the absence of anti-hebbian learning, especially if the input population had a 50:50 mix of peaked and monotonic gain fields. This work thus makes an important contribution to understanding how head-centred visual neurons may develop in the brain through an unsupervised process of visually-guided learning given visual precursor neurons with sigmoidal (monotonic) eye-position modulation. Furthermore, although we have studied one particular kind of coordinate transformation, i.e. from eye-centred to head-centred visual representations, these findings may also apply to a range of other coordinate transformations with sensorimotor integration of monotonically encoded motor variables [4, 5].

Supporting information

Appendix A.   Eye-centredness Reference Frame Analysis. During testing, the visual target was located in head-centred locations

$$t_j = t_1 + \Delta h(j-1) \tag{21}$$

for $j = 1, \ldots, T$, and while in each location it was observed from eye-positions

$$e_i = e_1 + \Delta e(i-1) \tag{22}$$

for $i = 1, \ldots, E$. The eye-position shift Δe was set to a multiple of the head-centred target location shift Δh to cause resampling of the neuron's response at the same retinal location for different eye-positions, thereby providing a resampling of the response in both head-centred and eye-centred space across multiple eye-positions.

The set of head-centred locations $\{t_1, \ldots, t_T\}$ corresponded to retinal locations $R_i = \{t_1 - e_i, \ldots, t_T - e_i\}$ when the model was fixating eye-position e_i, and from this it is clear that among retinal locations common to all eye-positions, $t_1 - e_1$ was the first and $t_T - e_E$ was the last, that is

$$\min \bigcap_i R_i = t_1 - e_1$$
$$\max \bigcap_i R_i = t_T - e_E \tag{23}$$

Therefore f_i and l_i, denoting the first and last position included from the ith response vector respectively, had to correspond to these two retinal locations respectively

$$t_{f_i} - e_i = t_1 - e_1 \tag{24}$$

$$t_{l_i} - e_i = t_T - e_E \tag{25}$$

We can resolve each equation to find an explicit formula for f_i and l_i in terms of i as follows.

By substituting Eq 21 and Eq 22 into Eq 24 we obtain

$$(t_1 + \Delta h(f_i - 1)) - (e_1 + \Delta e(i - 1)) = t_1 - e_1$$

Rearranging this gives

$$\Delta h(f_i - 1) - \Delta e(i - 1) = 0$$

$$f_i = \frac{\Delta e}{\Delta h}(i - 1) + 1 \tag{26}$$

By substituting Eq 21 and Eq 22 into Eq 25 we obtain

$$(t_1 + \Delta h(l_i - 1)) - (e_1 + \Delta e(i - 1)) = (t_1 + \Delta h(T - 1)) - (e_1 + \Delta e(E - 1))$$

Rearranging this gives

$$\Delta h(l_i - 1) - (e_1 + \Delta e(i - 1)) = \Delta h(T - 1) - (e_1 + \Delta e(E - 1))$$

$$\Delta h(l_i - 1) - \Delta e(i - 1) = \Delta h(T - 1) - \Delta e(E - 1)$$

$$\Delta h(l_i - 1 - (T - 1)) = -\Delta e(E - 1 + (i - 1))$$

$$\Delta h(l_i - T) = -\Delta e(E + i)$$

$$l_i = T - \frac{\Delta e}{\Delta h}(E + i) \tag{27}$$

We can also deduce the length V of the portion of each response vector that is used in the eye-centred correlation analysis as follows. By definition, for each response vector

$$V = l_i - f_i + 1$$

Substituting in Eq 26 and Eq 27 gives

$$V = T - \frac{\Delta e}{\Delta h}(E + i) - \left(\frac{\Delta e}{\Delta h}(i - 1) + 1\right) + 1$$

Rearranging gives

$$V = T - \frac{\Delta e}{\Delta h}(E + i) - \frac{\Delta e}{\Delta h}(i - 1)$$

$$= T - \frac{\Delta e}{\Delta h}(E + i - (i - 1))$$

$$= T - \frac{\Delta e}{\Delta h}(E + 1) \tag{28}$$

Acknowledgments

References

1. Mender BM, Stringer SM. A model of self-organizing head-centered visual responses in primate parietal areas. PloS one. 2013;8(12):e81406.

2. Andersen RA, Snyder LH, Li CS, Stricanne B. Coordinate transformations in the representation of spatial information. Current Opinion in Neurobiology. 1993;3(2):171–176.

3. Mender BM, Stringer SM. Self-organization of head-centered visual responses under ecological training conditions. Network: Computation in Neural Systems. 2014;25(3):116–136.

4. Xing J, Andersen RA. Models of the Posterior Parietal Cortex Which Perform Multimodal Integration and Represent Space in Several Coordinate Frames. Journal of Cognitive Neuroscience. 2000;12:601–614. doi:10.1162/089892900562363.

5. Chang SW, Papadimitriou C, Snyder LH. Using a compound gain field to compute a reach plan. Neuron. 2009;64(5):744–755.

6. Andersen RA, Mountcastle VB. The influence of the angle of gaze upon the excitability of the light-sensitive neurons of the posterior parietal cortex. The Journal of Neuroscience. 1983;3(3):532–548.

7. Andersen R, Essick G, Siegel R. Encoding of spatial location by posterior parietal neurons. Science. 1985;230(4724):456–458. doi:10.1126/science.4048942.

8. Andersen R, Bracewell R, Barash S, Gnadt J, Fogassi L. Eye position effects on visual, memory, and saccade-related activity in areas LIP and 7a of macaque. The Journal of Neuroscience. 1990;10(4):1176–1196.

9. Galletti C, Battaglini P, Fattori P. Eye Position Influence on the Parieto-occipital Area PO of the Macaque Monkey. European Journal of Neuroscience. 1995;7(12):2486–2501.

10. Mullette-Gillman OA, Cohen YE, Groh JM. Eye-Centered, Head-Centered, and Complex Coding of Visual and Auditory Targets in the Intraparietal Sulcus. Journal of Neurophysiology. 2005;94(4):2331–2352. doi:10.1152/jn.00021.2005.

11. Galletti C, Battaglini PP, Fattori P. Parietal neurons encoding spatial locations in craniotopic coordinates. Experimental Brain Research. 1993;96(2):221–229.

12. Duhamel JR, Bremmer F, BenHamed S, Graf W. Spatial invariance of visual receptive fields in parietal cortex neurons. Nature. 1997;389(6653):845–848.

13. Breveglieri R, Bosco A, Canessa A, Fattori P, Sabatini SP. Evidence for peak-shaped gaze fields in area V6A: implications for sensorimotor transformations in reaching tasks. In: Bioinspired Applications in Artificial and Natural Computation. Springer; 2009. p. 324–333.

14. Zipser D, Andersen RA. A back-propagation programmed network that simulates response properties of a subset of posterior parietal neurons. Nature. 1988;331(6158):679–684. doi:10.1038/331679a0.

15. Mazzoni P, Andersen RA, Jordan MI. A more biologically plausible learning rule for neural networks. Proceedings of the National Academy of Sciences. 1991;88(10):4433–4437.

16. Pouget A, Sejnowski TJ. Spatial Transformations in the Parietal Cortex Using Basis Functions. Journal of Cognitive Neuroscience. 1997;9:222–237. doi:10.1162/jocn.1997.9.2.222.

17. Pouget A, Snyder LH. Computational approaches to sensorimotor transformations. Nature Neuroscience. 2000;3 Suppl:1192–1198. doi:10.1038/81469.

18. Rolls ET, Treves A. Neural Networks and Brain Function. Oxford University Press Oxford; 1998.

19. O'Donohue TL, Millington WR, Handelmann GE, Contreras PC, Chronwall BM. On the 50th anniversary of Dale's law: multiple neurotransmitter neurons. Trends in Pharmacological Sciences. 1985;6(0):305 – 308. doi:http://dx.doi.org/10.1016/0165-6147(85)90141-5.

20. Salinas E, Abbott L. Transfer of coded information from sensory to motor networks. The Journal of Neuroscience. 1995;15(10):6461–6474.

21. Galletti C, Battaglini P, Fattori P. Functional Properties of Neurons in the Anterior Bank of the Parieto-occipital Sulcus of the Macaque Monkey. European Journal of Neuroscience. 1991;3(5):452–461.

22. Spratling MW. Learning posture invariant spatial representations through temporal correlations. Autonomous Mental Development, IEEE Transactions on. 2009;1(4):253–263.

23. Merriam EP, Gardner JL, Movshon JA, Heeger DJ. Modulation of visual responses by gaze direction in human visual cortex. Journal of Neuroscience. 2013;33(24):9879–9889.

24. Daddaoua N, Dicke P, Thier P. Eye position information is used to compensate the consequences of ocular torsion on V1 receptive fields. Nature communications. 2014;5:3047.

25. Rolls ET, Stringer SM. Invariant object recognition in the visual system with error correction and temporal difference learning. Network (Bristol, England). 2001;12(2):111–129.

26. Földiák P. Learning invariance from transformation sequences. Neural Computation. 1991;3(2):194–200.

27. Wallis G, Rolls ET. Invariant face and object recognition in the visual system. Progress in neurobiology. 1997;51(2):167–194.

28. Freedman EG, Sparks DL. Eye-head coordination during head-unrestrained gaze shifts in rhesus monkeys. Journal of Neurophysiology. 1997;77(5):2328–2348.

29. Dayan P, Abbott LF. Theoretical Neuroscience: Computational and Mathematical Modeling of Neural Systems. MIT Press, ISBN 0-262-04199-5; 2001.

30. Rolls ET. Invariant visual object and face recognition: neural and computational bases, and a model, VisNet. Frontiers in Computational Neuroscience. 2012;6(35).

31. Royer S, Paré D. Conservation of total synaptic weight through balanced synaptic depression and potentiation. Nature. 2003;422(6931):518–522.

32. Oja E. Simplified neuron model as a principal component analyzer. Journal of mathematical biology. 1982;15(3):267–273.

33. Kohonen T. Self-organization and associative memory. vol. 8. Springer Science & Business Media; 2012.

Input Population

Output Population

A

B

A UNTRAINED

PEAKED

Retina preference (deg)

Eye-position preference (deg)

B TRAINED

Retina preference (deg)

Eye-position preference (deg)

C

SIGMOIDAL

Retinal preference (deg)

Eye position preference (deg)

D

Retinal preference (deg)

Eye position preference (deg)

Legend:
- Peaked untrained
- Peaked trained
- Sigmoidal untrained
- Sigmoidal trained

Axis labels: Eye Centeredness (x-axis), Head Centeredness (y-axis)

A

Retinal preference (deg) — 100, 80, 60, 40, 20, 0, 20, 40, 60, 80, 100

Eye-position preference (deg) — 30 15 0 15 30

Colorbar: 0, 10, 20, 30, 40, 50, 60, 70, 80, 90, 100

B

Retinal preference (deg) — 100, 80, 60, 40, 20, 0, −20, −40, −60, −80, −100

Eye-position preference (deg) — −30−15 0 15 30−15 0 15 30

Colorbar: 0, 50, 100, 150, 200, 250

A HEBBIAN

Retina preference (deg)

Eye-position preference (deg)

B TRACE

Retina preference (deg)

Eye-position preference (deg)

PEAKED

C

Retinal preference (deg)

Eye position preference (deg)

D

Retinal preference (deg)

Eye position preference (deg)

SIGMOIDAL

K>0   K<0

r=h+E/2

A

r=h-e

B

r=h-e

h

0

r=h-E/2

Retinal Location - r (deg)

0   0

Eye position - e (deg)

A

Legend
Head comminress rate
Avg Head comminress
Avg Eye comminress

B

A UNTRAINED

Firing Rate vs. Head–Centred Location (deg)

Legend:
- Fixating −18°
- Fixating −6°
- Fixating 6°
- Fixating 18°

B TRAINED

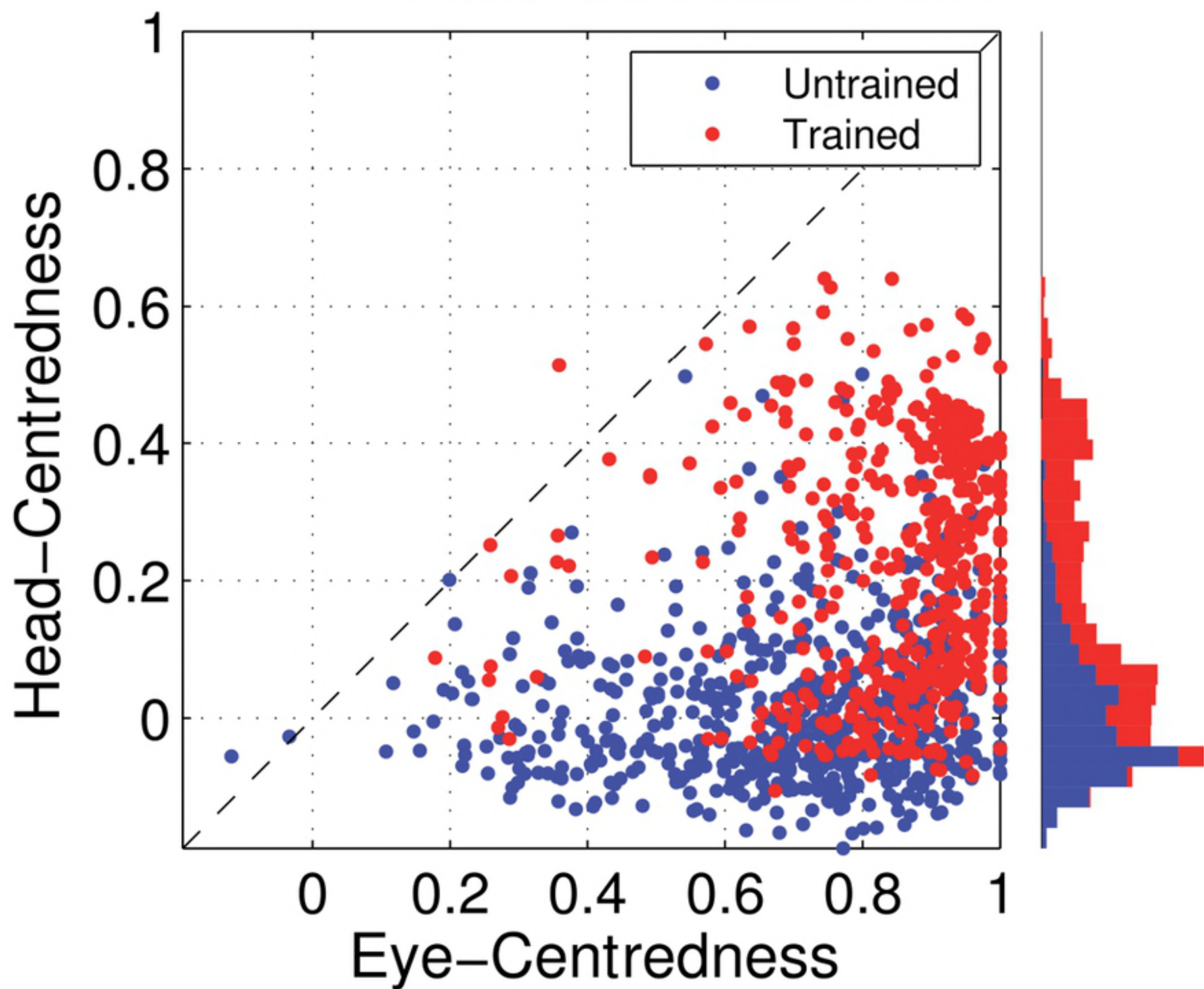Firing Rate vs. Head–Centred Location (deg)

Legend:
- Fixating −18°
- Fixating −6°
- Fixating 6°
- Fixating 18°

A UNTRAINED

B TRAINED

Retinal preference (deg)

Eye-position preference (deg)

A UNTRAINED

B TRAINED

Firing Rate — Head-Centred Location (deg)

Fixating −18°
Fixating −6°
Fixating 6°
Fixating 18°

A UNTRAINED

B TRAINED

Retinal preference (deg)

Eye−position preference (deg)

A UNTRAINED

B TRAINED

Firing Rate vs. Head-Centred Location (deg)

Legend (A): Fixating −18°, Fixating −6°, Fixating 6°, Fixating 18°

Legend (B): Fixating −18°, Fixating −6°, Fixating 6°, Fixating 18°

A UNTRAINED

B TRAINED

A UNTRAINED

B TRAINED

Firing Rate

Head–Centred Location (deg)

Fixating −18°
Fixating −6°
Fixating 6°
Fixating 18°

A UNTRAINED

B TRAINED

A UNTRAINED

B TRAINED

Firing Rate

Fixating −18°
Fixating −6°
Fixating 6°
Fixating 18°

Head-Centred Location (deg)

A UNTRAINED

Retinal preference (deg)

Eye-position preference (deg)

B TRAINED

Retinal preference (deg)

Eye-position preference (deg)

A UNTRAINED

B TRAINED

PEAKED

Firing Rate

Firing Rate

Fixating −18°
Fixating −6°
Fixating 6°
Fixating 18°

Head−Centred Location (deg)

C

D

SIGMOIDAL

Firing Rate

Firing Rate

Fixating −18°
Fixating −6°
Fixating 6°
Fixating 18°

Head−Centred Location (deg)